



Transient landscape evolution of basement-cored uplifts: Example of the Kyrgyz Range, Tian Shan

Michael E. Oskin¹ and Douglas Burbank²

Received 5 May 2006; revised 17 February 2007; accepted 6 April 2007; published 15 August 2007.

[1] The Kyrgyz Range, located on the northern margin of the western Tian Shan, illustrates long-term (10^6 – 10^7 year) transient landscape evolution in response to an active basement-cored rock uplift. Eastward propagation of range uplift has progressively exposed resistant bedrock capped by a tilted, (formerly) planar, pre-Cenozoic unconformity. We develop an approximate, stream power–based analytic model of transient river profile incision into progressively exposed and resistant bedrock to explore the patterns of channel development into the unconformity surface. This analysis shows that the unconformity can be preserved as a geomorphic marker defined by upland headwaters and interfluvial areas. Though channels are not at equilibrium with rock uplift, prominent knickpoints are not predicted to develop on main stem channels. However, knickpoints are predicted to develop on tributaries upstream of their junctions with the trunk stream because of differential erosion rates. Initial channel slope and transient channel form are both sensitive to the n value of the stream power model and could prove useful for calibration of n from field data. Accumulation of catchment area (a proxy for discharge) into larger catchments develops a positive feedback where larger drainages with higher stream power at a given slope undermine and capture adjacent drainage area. A simple model of competitive fluvial incision illustrates the role of tributary junction position in maximizing stream power expended upon the trunk stream. Examples from the Kyrgyz Range illustrate the effects of tributary junction position on fluvial relief, and we propose that adjustments to the tributary network through stream capture are ongoing within this landscape even after several kilometers of exhumation.

Citation: Oskin, M. E., and D. Burbank (2007), Transient landscape evolution of basement-cored uplifts: Example of the Kyrgyz Range, Tian Shan, *J. Geophys. Res.*, 112, F03S03, doi:10.1029/2006JF000563.

1. Introduction

[2] Fluvial relief, i.e., the relief conveyed by bedrock channels, is the primary control on the overall topographic relief in mountainous landscapes [Whipple *et al.*, 1999]. Under equilibrium conditions, where fluvial bedrock incision balances rock uplift, bedrock channel profiles develop a predictable concave longitudinal profile [Whipple and Tucker, 1999]. However, channel networks that erode bedrock and convey sediment away from a growing uplift are not born into an equilibrium condition. Nascent uplifts disrupt preexisting drainage networks, build elevation, and establish new topographic divides [Humphrey and Konrad, 2000; Sobel *et al.*, 2003]. Where exhumation of low-erosivity basement promotes development of steep channel gradients, formation of high topography may inhibit fault slip and drive tectonic shortening elsewhere before equilibrium conditions can be established [Molnar and Lyon-Caen,

1988; Hilley *et al.*, 2005]. Thus, in order to predict the topographic evolution of a growing orogen, the evolution of bedrock river channel profiles must be examined under disequilibrium, or transient conditions. In addition, the arrangement of entire channel networks and sizes of catchments also evolve within a growing uplift [Densmore *et al.*, 2004, 2005]. These processes, which affect the downstream accumulation of discharge in a landscape, can have a significant impact on fluvial relief because of the tradeoff of channel slope and discharge as channel profiles approach equilibrium grade [Howard, 1994].

[3] In this paper we examine the transient development of river longitudinal profiles into a basement block undergoing surface uplift. This contribution is motivated by observations of the Kyrgyz Range, a field example of an actively growing basement-cored range from the northwestern margin of the Tian Shan orogen (Figure 1). Rather than develop a comprehensive model of all surface processes that affect a growing basement massif, we instead isolate two first-order processes that modulate the evolution of transient river channel longitudinal profiles and explore these analytically. The advantage of this approach is that we gain insight into the specific relationship between parameters controlling erosion and development of transient channel longitudinal

¹Department of Geological Sciences, University of North Carolina at Chapel Hill, Chapel Hill, North Carolina, USA.

²Department of Earth Science, University of California, Santa Barbara, California, USA.

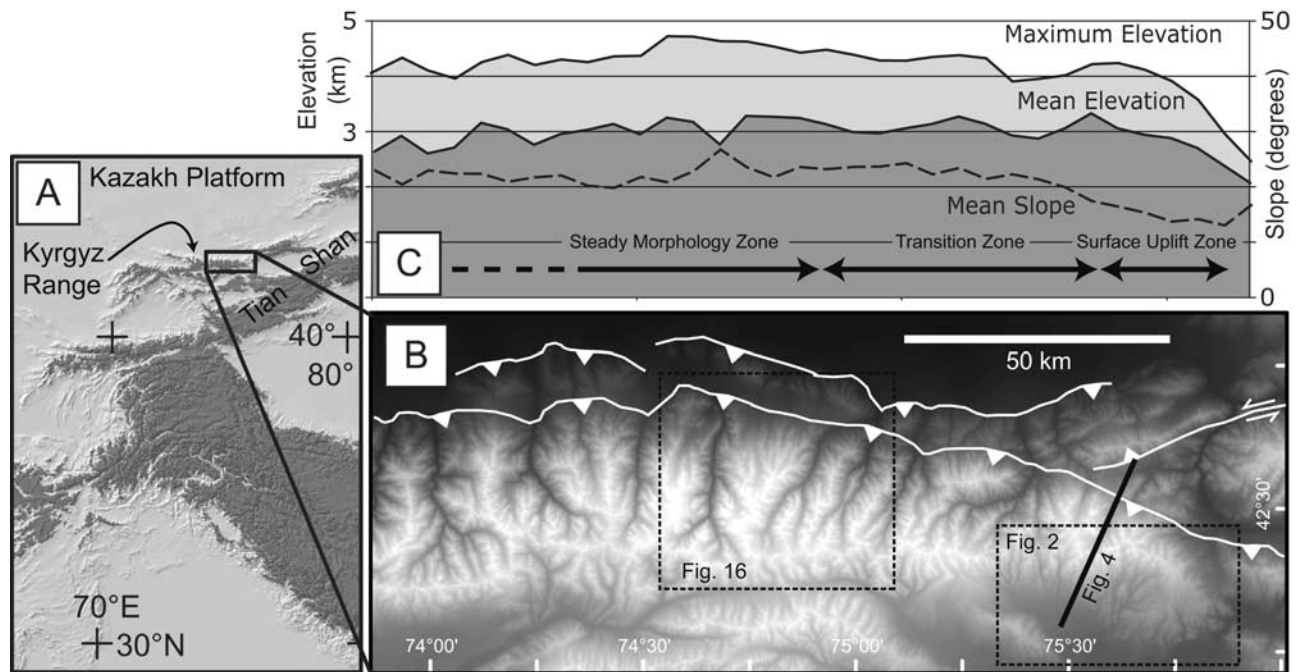


Figure 1. (a) Shaded relief map of central Asia. Shaded areas show elevations over 3 km. Kyrgyz Range is an active basement-cored range where the northern margin of the Tian Shan orogen overthrusts the Kazakh Platform. (b) Shuttle Radar Topography Mission digital elevation data from eastern half of Kyrgyz Range. Active reverse faults are shown as white lines. (c) Graph of maximum elevation, mean elevation, and mean slope angle in 10-km-wide bins for the eastern and central Kyrgyz Range. Horizontal axis corresponds to landscape in Figure 1b. Also shown are surface uplift, transition, and steady state zones as defined by *Sobel et al.* [2006]. Rising peak elevations in surface uplift zone are not accompanied by significant incision of canyons. Significant enlargement and deepening of canyons occurs in the transition zone with relief development driving steepening of hillslopes.

profiles. We begin by introducing the Kyrgyz Range study area. Next we review the stream power–based erosion rule [Howard and Kerby, 1983] and develop a kinematic wave–based solution for an equilibrium channel profile for the case where channel incision rate is linear with channel slope. We then extend this solution to approximate transient cases where incision rate is nonlinear with slope and apply this solution to model transient river profiles developed on a tilted, progressively exposed resistant bedrock surface. These surfaces develop during exposure of the unconformity that separates easily erodible sedimentary rocks from resistant basement and are common features of basement-involved orogens, including much of the Tian Shan [Davis, 1904; Burbank et al., 1999; Abdrakhmatov et al., 2001], the Sierra Pampeanas [Jordan and Allmendinger, 1986], the Rocky Mountains [Gregory and Chase, 1994], and southern California [Spotila et al., 1998]. Our analytic model lends insight into the conditions necessary to preserve a relict “surface” in the landscape and reveals a pattern of knickpoints developed at tributary junctions that should be a characteristic feature of these landscapes. We also find that the pattern of channel incision is strongly affected by the nonlinearity of the dependence of incision rate on slope. This dependence, which can be directly related to the incision process [Hancock et al., 1998; Whipple et al., 2000; Tucker and Whipple, 2002], is difficult to uniquely extract from equilibrium channel gradients [Whipple and Tucker, 1999]. Next we explore the amalgamation of

catchment area into larger drainage basins with progressive incision into a basement-cored uplift [Densmore et al., 2004, 2005]. We model this process via competitive fluvial incision of adjacent tributaries and develop the role of positive feedback between catchment area and channel incision to drive stream capture. Stream capture may occur through undermining of adjacent catchments and rerouting of tributaries, or possibly through gradual adjustment of the positions of tributary junctions within the landscape [Howard, 1971]. Steepened “knickzones” that form on the trunk stream ahead of tributary junctions may be evidence of recent or ongoing stream capture processes.

[4] This contribution does not develop a complete model for landscape evolution in basement-cored uplifts, but rather focuses on first-order processes expressed at two different stages of range development. A comprehensive landscape evolution model would require further consideration of the interactions among these processes as well as additional phenomena not considered here. For example, development of threshold hillslopes [Burbank et al., 1996] occurs in concert with relief production. The role of sediment production from these hillslopes and its potential effects on bedrock channel incision [Sklar and Dietrich, 1998, 2004] are not considered. Also, surface uplift of erosionally resistant basement rocks results in landscapes that cross disparate climate zones and leads to both positive and negative reinforcement of precipitation and its effects on the landscape. For example, the Kyrgyz Range encompasses

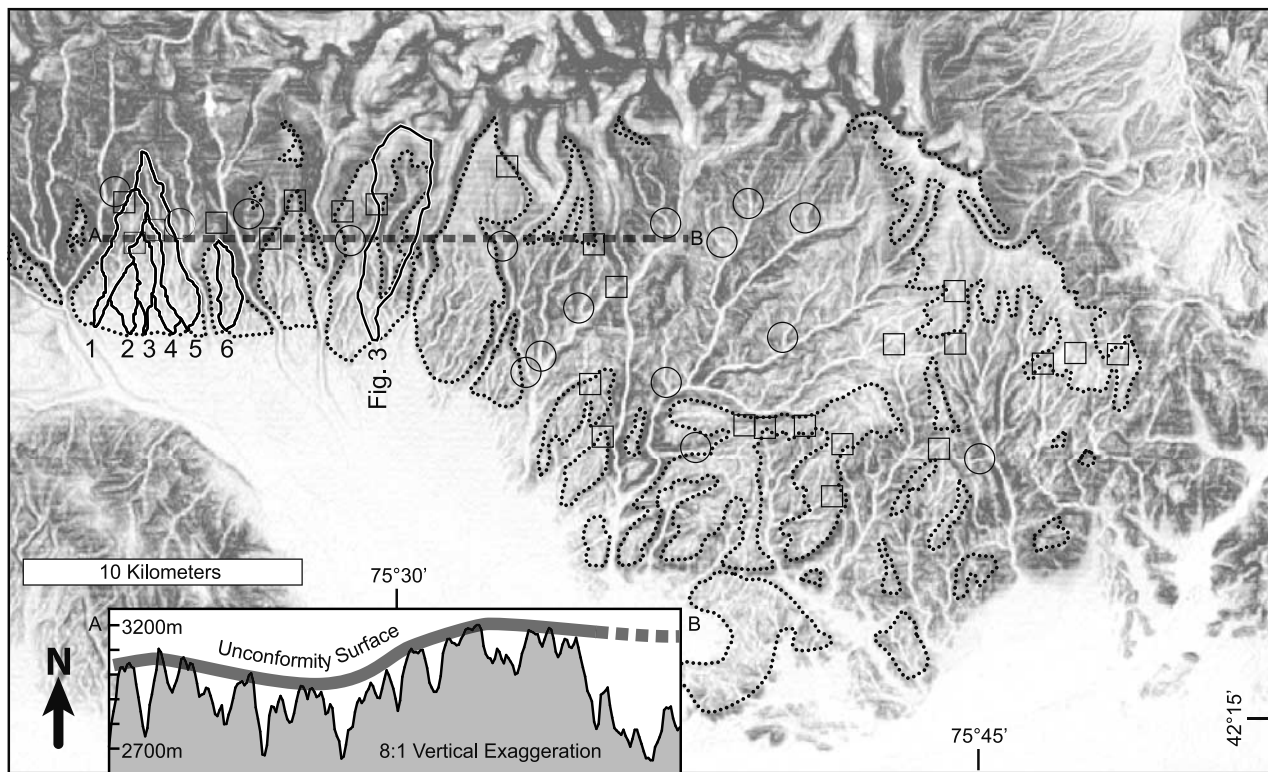


Figure 2. Slope map calculated along steepest descent showing steep slopes that separate canyons from medium-slope upland surfaces and lower-slope channels. Darker areas correspond to steeper slopes. Slopes are derived from 90 m Shuttle Radar Topography Mission digital elevation data. Domain of relict surfaces, outlined by dotted lines, is clearly distinguished from zone of glacial erosion (wide valleys with steps and steep cirque headwalls) and fluvially modified landscapes (steep canyon walls, narrow canyon floors with low gradient, and knife-edge ridges). Channel profiles from catchments 1 through 6 are analyzed in Figure 11. Open circles show locations of prominent knickpoints developed at tributary junctions. Open squares show locations of beheaded streams where upstream areas have been captured by adjacent catchments. Cross section A-B shows gently undulating unconformity surface defining concordant low-relief upland surfaces. Note that the 8:1 vertical exaggeration enhances amplitude of undulation of the surface.

nearly 4 km of topographic relief (Figure 1) from the Kazakh platform (800 m) to its highest peaks (4,700 m). Annual precipitation generally increases with elevation, but winter cyclonic storm systems dominate at low elevations while summer convective storms become more important sources of rain and snow at high elevation [Aizen *et al.*, 1995]. These orographic effects are not considered in the transient channel profile evolution models developed here.

2. Study Area

[5] The Kyrgyz Range, the northernmost range of the Kyrgyzstan Tian Shan (Figure 1), provides a natural laboratory to examine the erosional processes that develop relief and balance rock uplift in basement-cored orogens. The Kyrgyzstan Tian Shan absorb up to 13 mm/yr of shortening distributed across a series of basement-cored ranges and intrabasinal faults [Abdrakhmatov *et al.*, 1996; Thompson *et al.*, 2002]. Approximately 1.5 mm/yr of this shortening occurs at the foot of the Kyrgyz Range, which defines the accretionary boundary between the high topography of the

Tian Shan and the stable, low-elevation Kazakh platform [Bullen *et al.*, 2001, 2003; Thompson *et al.*, 2002].

[6] Concordant, low-relief surfaces underlain by erosion-resistant Paleozoic metamorphic and plutonic basement rocks characterize the crests and slopes of many ranges within the western Tian Shan [Davis, 1904; Chediya, 1986; Burbank *et al.*, 1999; Abdrakhmatov *et al.*, 2001], including the easternmost 50 km of the south facing range slope of the Kyrgyz Range [Oskin and Burbank, 2005] (Figure 2). These basement surfaces are coincident with the unconformable basal contact of unconsolidated Cenozoic nonmarine sedimentary rocks and are interpreted as exposed, folded remnants of this contact surface [Burbank *et al.*, 1999]. Because Late Cenozoic syntectonic strata are removed, the elevation of this “unconformity surface” with respect to the stable Kazakh platform defines, to first order, the net rock uplift and shortening of the western Tian Shan [Abdrakhmatov *et al.*, 2001].

[7] The Kyrgyz Range preserves the transition from a presteady state condition where surface uplift dominates and erosion is minimal, to a condition that at least approaches a flux steady state [Willett and Brandon, 2002] where the

Table 1. Explanation of Symbols Used in Text

Symbol	Name	Units
$A(x)$	catchment area	m^2
C	capture point	m
E	channel erosion rate	$m\ yr^{-1}$
ϵ	finite erosion	m
h	Hack exponent	
θ	concavity	
$K = K_e K_d^n K_a^{n\theta}$	combined constant	$m^{1-p}\ yr^{-1}$
K_a	Hack constant	m^{2-h}
K_d	dimensional constant	$J\ m^{-2(\theta+1)}\ yr^{-1}$
K_e	erodibility	$J^{-n}\ m^{2n+1}\ yr^{n-1}$
L	catchment length	m
$m = n\theta$	area exponent	
n	slope exponent	
$p = hn\theta$	distance exponent	
S_0	initial channel slope	
S_c	present channel slope	
t	time	years
$t_i(z)$	time of initial channel position	years
Δt	finite time	years
$U(x), U$	rock uplift rate	$m\ yr^{-1}$
U_0, U_1	$U(x)$ coefficients	$m\ yr^{-1},\ yr^{-1}$
V	vertical rate of exposure	$m\ yr^{-1}$
W	catchment width	m
x	distance downstream	m
$x_i(z)$	initial channel position	m
x_c	channel head position	m
Δx	finite distance	m
z	elevation	m
z_o	elevation of divide	m
Δz	finite elevation	m

erosion rate balances the rock uplift rate [Sobel *et al.*, 2006]. Over 5 km of erosion of the central, highest-relief portion of the Kyrgyz Range has occurred, sufficient to completely remove the unconformity surface and exhume apatite with reset fission track ages [Bullen *et al.*, 2001]. Additional apatite fission track data from the eastern half of the range indicate that total exhumation increases from east to west along the range crest. These data further support that this gradient in exhumation has evolved over time, with over 110 km of lateral propagation of the range tip over the last 8 to 11 Ma [Sobel *et al.*, 2006]. Trends in rock uplift and exhumation in the eastern part of the range are correlated to the growth and stabilization of range elevation, deepening of relief of incised canyons, and rising average hillslope angles (Figure 1). These metrics gradually approach spatially average values at the center of the range, suggesting that further topographic adjustments are not required to balance rock uplift. These data support our contention that the evolution of range-scale steady state topography of the Kyrgyz Range may be examined in the context of a space-for-time substitution, where systematic spatial topographic patterns inform our understanding of the temporal development of geomorphology at a site within the range.

[8] We closely examine two aspects of the presteady state topographic evolution of channel profiles in the Kyrgyz Range. We first consider observations at the foot of the Kyrgyz Range that highlight disparate regimes of bedrock channel incision upon exposure of the unconformity (Figure 2). New channels incise interfluvial regions to develop a dense channel network characterized by low interfluvial relief. These areas form relict surfaces in the landscape

that are separated by deeply incised gorges connected to larger drainage areas higher up in the range. Second, we consider the continued evolution of channel networks in more deeply incised portions of the landscape. Here we develop a mechanism that relies on competitive fluvial incision to promote the observed gradual consolidation of drainage area into fewer, but larger catchments (Figure 1).

3. Stream Power Analytic Model

[9] To explore the form of channel profiles we relate channel erosion rate to channel slope and upstream catchment area through a general form of the stream power erosion rule [Howard and Kerby, 1983], where the rate of change in elevation of the surface,

$$\frac{dz}{dt} = U(x) - K_e \left[K_d A(x)^\theta \left| \frac{dz}{dx} \right|^n \right]. \quad (1)$$

$U(x)$ is the rock uplift rate relative to a datum, which may either be local base level or a global reference frame, such as the geoid [England and Molnar, 1990]. Equation (1) may be cast to represent mechanisms and transient behavior of a range of possible bedrock channel incision models [Howard, 1994; Whipple and Tucker, 1999, 2002; Lague *et al.*, 2005] and may be readily manipulated analytically [Whipple and Tucker, 1999; Humphrey and Konrad, 2000] to produce theoretical channel profiles [Whipple *et al.*, 1999]. Erosive power is spatially controlled by downstream slope of the channel bed, $\left| \frac{dz}{dx} \right|$ and the upstream drainage basin area, A , as a proxy for the effective discharge. The intrinsic concavity, θ , expresses the geometry of the longitudinal bedrock channel and the scaling of effective discharge with drainage basin size, including possible orographic increase in precipitation with elevation [Roe *et al.*, 2003]. The exponent n relates to the erosion mechanism [Hancock *et al.*, 1998; Whipple *et al.*, 2000] and the effect of a distribution of discharge events [Snyder *et al.*, 2003; Lague *et al.*, 2005]. At steady state and with a spatially uniform erosion rate, θ may be empirically estimated from the concavity of channel profiles [Whipple and Tucker, 1999] and is approximately 0.5 for bedrock channels [Howard, 1994]. Note that the product, $n\theta$, is commonly combined into the exponent m in other studies [Howard, 1994; Whipple and Tucker, 1999; Kirby and Whipple, 2001; Snyder *et al.*, 2003]. The coefficient, K_d , collects physical constants of gravity and the density of water as well as dimensional constants from derivation of either unit stream power or shear stress at the river bed in terms of upstream drainage area. We cast the units of the term inside the brackets as unit stream power in $J/m^2/yr$. K_e represents the resistance of the channel substrate to erosion and its units convert those of unit stream power to the exponent, n , into an erosion rate in m/yr . The actual units of K_d and K_e depend upon the exponents θ and n (Table 1).

[10] The distribution of erosive power along the length of a channel is strongly related to the downstream increase in basin size, A . Montgomery and Dietrich [1992], expanding on work by Hack [1957], documented that globally, drainage basin size scales with the square of distance downstream. Discharge increases downstream in these “box-like” basins primarily via accumulation of tributary streams. Many of the

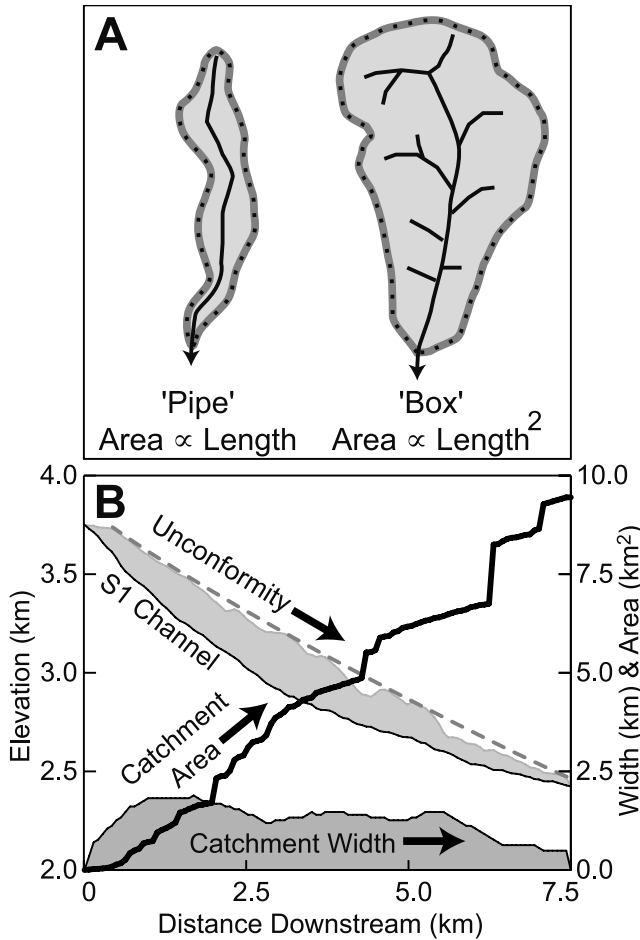


Figure 3. (a) Plan view illustration of “pipe-like” catchments where discharge increases linearly with distance downstream versus “box-like” catchments where catchment area increases with the square of distance downstream. Catchment area is a proxy for discharge in the stream power law. (b) Example of a “pipe-like” catchment from the south facing slope of the Kyrgyz Range. Unconformity surface defines ridge line elevations. Maximum incision of channel floor is <500 m below this surface. Catchment width remains approximately constant downstream, while drainage area on the trunk stream increases linearly with distance.

channels draining the southeastern Kyrgyz Range do not display this scaling relationship. Rather, these basins are intermediate between “box-like” and “pipe-like” in form (Figure 3); they lack significant tributaries, and drainage basin size scales less strongly with downstream distance. The relationship,

$$A(x) = K_a x^h, \quad (2)$$

which is the inverse of Hack’s Law [Hack, 1957], captures the growth of basin size, A , with channel-wise distance downstream, x , and scaling with h ranging typically from 1 (pipe-like) to 2 (box-like).

[11] For the steady state case where erosion rate everywhere equals rock uplift rate, elevation drop along an equilibrium channel is derived by substituting (2) into (1), setting $\frac{dz}{dt}$ to zero, and integrating downstream from the channel head at x_c [Whipple and Tucker, 1999],

$$z(x) = \int_{x_c}^x \left(\frac{U(x)}{K_e} \right)^{\frac{1}{n}} \frac{1}{K_d K_a^{\theta}} x^{-h\theta} dx. \quad (3)$$

For the case where $U(x)$ is a constant, U , and $h\theta \neq 1$,

$$z(x) = \left(\frac{U}{K_e} \right)^{\frac{1}{n}} \frac{1}{K_d K_a^{\theta} (1 - h\theta)} (x^{1-h\theta} - x_c^{1-h\theta}). \quad (4)$$

Under equilibrium conditions, the only dependence on n comes from the ratio of uplift rate, $U(x)$, to erodibility, K_e . Kirby and Whipple [2001] exploited this dependence to derive $n = 1$ from channel profiles across portions of the Siwalik Hills with varying $U(x)$. However, it is generally difficult to extract n values from equilibrium channel profiles because of other conditions, such as the erodibility, K_e , may also vary between sites with different $U(x)$ [Snyder et al., 2000].

[12] Our analysis of disequilibrium, or transient channel profiles builds upon an alternative, kinematic wave solution to (1). We combine (1) and (2) and substitute $p = hn\theta$ and $K = K_e K_d^n K_a^{n\theta}$ to yield a formula for elevation change with respect to channel-wise distance,

$$\frac{dz}{dt} = U(x) - Kx^p \left| \frac{dz}{dx} \right|^n, \quad (5)$$

where x is positive downstream. For the time being we drop the $U(x)$ term and only consider elevation change due to erosion. Rock uplift rate, or another description of differential rock uplift, is incorporated later as an initial condition to the solutions to (5) presented here. By multiplying each side by $\frac{dx}{dz}$ we rearrange (5) into a kinematic wave equation in the x direction,

$$\frac{dx}{dt} = -Kx^p \left| \frac{dz}{dx} \right|^{n-1}. \quad (6)$$

[13] Whipple and Tucker [1999] derived (6) to describe the kinematic wave speed, or celerity, of knickpoint propagation in the upstream, negative x direction. We note that (6) more generally describes the upstream rate of backwearing of all positions, $x(z)$, on a channel. This rate may be integrated for the $n = 1$ case to solve for the channel position at any time, $x(z, t)$. For the $n \neq 1$ case, we substitute the absolute value of initial channel slope, S_0 , for $\frac{dz}{dx}$ to explore the initial stages of transient channel profile evolution where channel slope does not change significantly. The resulting differential equation is an initial value problem solved by separation of variables,

$$\int x^{-p} dx = -KS_0^{n-1} \int dt. \quad (7)$$

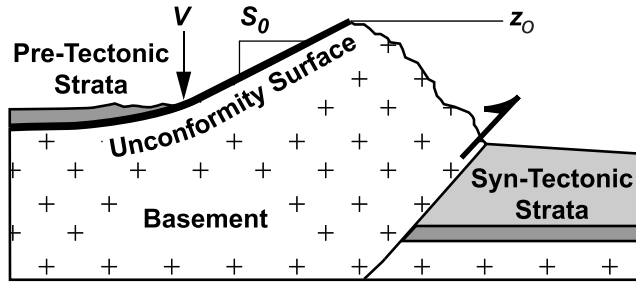


Figure 4. Initial conditions of transient channel profile incision into progressively exposed unconformity surface. Here z_0 is the elevation of the divide, S_0 is the slope of the unconformity surface, and V is the vertical rate of exposure of the tilted unconformity surface.

Integration of (7) yields the general solution,

$$x(z, t) = \left[x_i(z)^{1-p} - KS_0^{n-1} (1-p)(t - t_i(z)) \right]^{\frac{1}{1-p}}, \quad p \neq 1, \quad (8)$$

$$x(z, t) = x_i(z) e^{-KS_0^{n-1}(t-t_i(z))}, \quad p = 1, \quad (9)$$

where $x_i(z)$ prescribes a point through which the solution must pass at time $t_i(z)$. Because both of these initial conditions may vary as a function of elevation, z , these can describe moving boundaries, such as uplift of rocks relative to base level, $U(x)$. It is important to keep in mind that (8) and (9) are strictly solutions only for the $n = 1$ case. Where $n \neq 1$, these equations only approximate the initial stages of channel profile evolution where channel slope is not much changed from S_0 .

[14] To illustrate that (8) is indeed a solution for the $n = 1$ case, we use this solution to derive an equilibrium channel profile and compare this to the result from (4). The key to this comparison lies in the selection of the initial conditions. We choose to track particles of rock that pass through the channel head at $(x = x_c, z = 0)$. Because at equilibrium, rock uplift is balanced by erosion, the time that a particle of rock at a depth, $-z$, reaches the channel head position is prescribed by the sum of the present time, t , and the depth divided by the uplift rate, $-z/U$. The set of initial conditions are thus completely described by

$$x_i(z) = x_c \quad (10)$$

$$t_i(z) = t - \frac{z}{U}. \quad (11)$$

[15] Substituting these into (8),

$$x(z, t) = \left[x_c^{(1-p)} - K(1-p)(t - t + z/U) \right]^{1/(1-p)}. \quad (12)$$

[16] The dependence on t disappears so that (12) can be rearranged to solve for $z(x)$,

$$z(x) = \left(\frac{U}{K(1-p)} \right) (x^{1-p} - x_c^{1-p}), \quad (13)$$

which is identical to (4) for $n = 1$, $p = h\theta$, and $K = K_e K_d K_a^\theta$.

4. Transient Channel Incision Into a Tilted Surface

4.1. Analytic and Numerical Model

[17] The utility of equations (8) and (9) lies in the flexibility of the initial conditions to model tectonic processes that vary over x and t . In this section we develop a model for channels that continually evolve their profiles during incision into a tilted, progressively exhumed, and resistant lithology. This model simultaneously explains both deep incision and exhumation of relict, tilted surfaces that maintain the essence of their initially planar form in the landscape. We consider exact solutions for the linear $n = 1$ case as well as approximate solutions for the nonlinear $n \neq 1$ case.

[18] Channel incision into a progressively exposed, tilted unconformity surface is controlled by V , the rate of exposure in the z direction (equal to the erosion rate through the sedimentary cover), and the tilt angle of the surface, S_0 (Figure 4). These determine initial conditions $x_i(z)$ and $t_i(z)$ with respect to a reference elevation at $z(x = 0, t = 0)$, z_0 ,

$$x_i(z) = \frac{z_0 - z}{S_0} \quad (14)$$

$$t_i(z) = \frac{z_0 - z}{V}. \quad (15)$$

[19] Solutions to (8) or (9) are defined by a starting elevation, z_0 , and the time elapsed since the channel began to incise below the unconformity, $t = z_0/V$. S_0 and V are fixed (Figure 4). Positions $z(x)$ are derived by iteratively solving (8) or (9) for z at each position x . For cases where $p \geq 1$, lowering of the headwaters position at $x = 0$ is either zero or undefined, but effectively zero. However, lowering of the headwaters position can be significant for $p < 1$ because portions of the channel downstream can erode back to the headwaters position.

[20] Solutions to (8) at different times show a strong imprint of initial conditions on the transient evolution of channel incision (Figure 5). As resistant rocks are exposed, channels gradually incise increasingly concave profiles. These transient profiles develop via the tradeoff between incision time and stream power with progressive exposure of resistant bedrock. Rather than develop a knickpoint, as expected in the case of uniform block uplift [Whipple and Tucker, 1999], the channel continuously evolves as it retreats into the landscape. The imprint of the initially planar unconformity surface persists so long as the rate of exposure of the unconformity, V , is significantly greater than the channel incision rate at the base of the lengthening channel profile.

[21] Recasting the solutions to (8) with channels that begin to incise beneath the unconformity at different positions within a landscape lends insight into the origin of relict surfaces defined by concordant interfluves (Figure 5b). Where a smaller stream commences incision beneath the

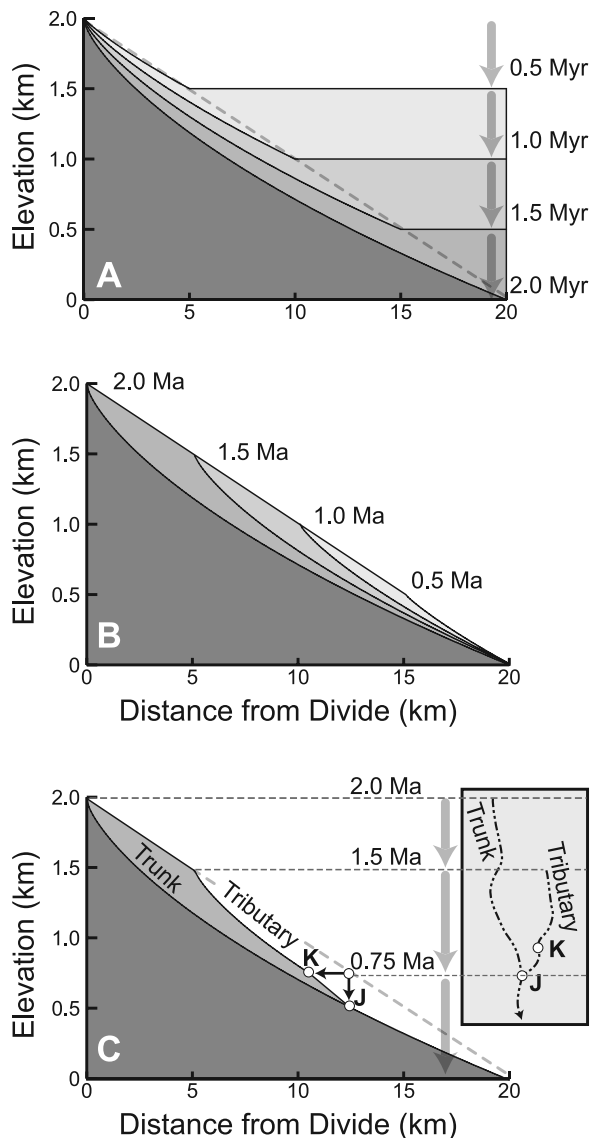


Figure 5. Solutions for incision of transient stream profiles with $h = 1.5$, $n = 1$, and $\theta = 0.5$. (a) Solutions shown for channels developed at different times into progressively exposed resistant bedrock surface. Arrows on right side of plot depict gradual removal of cover rocks from the unconformity. Differently shaded bands depict rock removed at each time step. Dashed line is the position of the unconformity. (b) Solution as in Figure 5a but with channels starting at later times as the unconformity is progressively exposed. Differently shaded bands show differential erosion between channels. (c) Solution for a trunk stream that begins incising below the unconformity at 2.0 Ma and a tributary that begins at 1.5 Ma. Arrows depict gradual removal of cover rocks, and horizontal lines tie stream profiles to positions in map view, at right. Inclined dashed line is the position of the unconformity. The tributary junction, point J, begins to incise below the unconformity at 0.75 Ma. Incision at the junction is paced by the more rapid incision rate of the trunk stream, leading to formation of a knickpoint that retreats up the tributary stream to point K. For the $n = 1$ case shown here, the position of this knickpoint is set by the elevation where the tributary junction began to incise below the unconformity.

unconformity at a lower elevation, incision of an adjacent larger stream consistently outpaces the smaller over time. If the smaller stream is joined as a tributary to the larger stream, then its conditions change following exposure of the unconformity at the junction. Because of the abrupt increase in incision rate across the junction, a knickpoint will develop on the tributary immediately upstream of the junction (Figure 5c). As incision progresses, this steeper reach expands into the tributary catchment as a knickzone (KJ on Figure 5c). For the case of $n = 1$, where knickpoint retreat rate is proportional only to catchment area, these developing knickzones will grow at a near-uniform slope determined by the ratio of catchment areas of the tributary and trunk stream. The elevation of the knickpoint (K on Figure 5c) is pinned to the elevation where the tributary junction intersected the unconformity. For cases where $n \neq 1$, the upper part of the knickzone will retreat more rapidly into the tributary [Tucker and Whipple, 2002]. This could make these knickzones increasingly difficult to recognize as incision progresses. Small catchment areas in low-order streams retard the rate of propagation of knickpoints such that low-gradient upland portions of the tributary network persist in the landscape [Whipple and Tucker, 1999; Crosby and Whipple, 2006; Wobus et al., 2006]. Because all transient low-order tributary streams at a given elevation begin incising resistant rocks simultaneously as the unconformity surface is exposed, the adjacent catchments together define an upland surface of low relief with a regional slope that mimics the original unconformity position.

[22] Basin geometry plays an important role in preserving the imprint of the exhumed unconformity surface. At a given erodibility and rate of exposure, proportionally greater lengthening of “pipe-like” basins than “box-like” basins (Figure 3) is required to reach the critical drainage size such that erosion balances the exposure rate of the unconformity surface, V . Solutions for different values of h scaled such that basin areas are identical at $x = 10$ km show that more “box-like” basins, with $h = 1.5$ and $h = 2$, develop more symmetrical upstream and downstream profiles than “pipe-like” basins with $h = 1$ (Figure 6). This occurs because stream power is proportionally diminished in upstream positions and enhanced in downstream positions for $h > 1$. For cases where basins are “pipe-like,” nearly uniform rates of lowering of headwaters regions can preserve linear interfluvial regions even with significant incision beneath the original unconformity position (Figure 6, top). These interfluvial regions may define an apparent surface with a slope somewhat less than the original unconformity slope.

[23] Transient stream profiles developed with variable n and fixed $h = 1$ (Figure 7) vary in a similar manner to the solutions presented with fixed n and variable h (Figure 6). This similarity arises because both n and h are exponents of distance in (5). Though solutions are only approximate for $n \neq 1$, numerical simulations of (1) with initial conditions defined by (14) and (15) show that the approximation is appropriate for low amounts of total erosion and n values close to 1 (Figure 8). However, the approximation does not adequately represent erosion rates for larger values of n , and thus the stream profiles presented for $n = 3$ significantly overpredict erosion at downstream positions. In order to develop landscapes dominated by the relict imprint of the unconformity at similar length scales, erodibility values, K_e ,

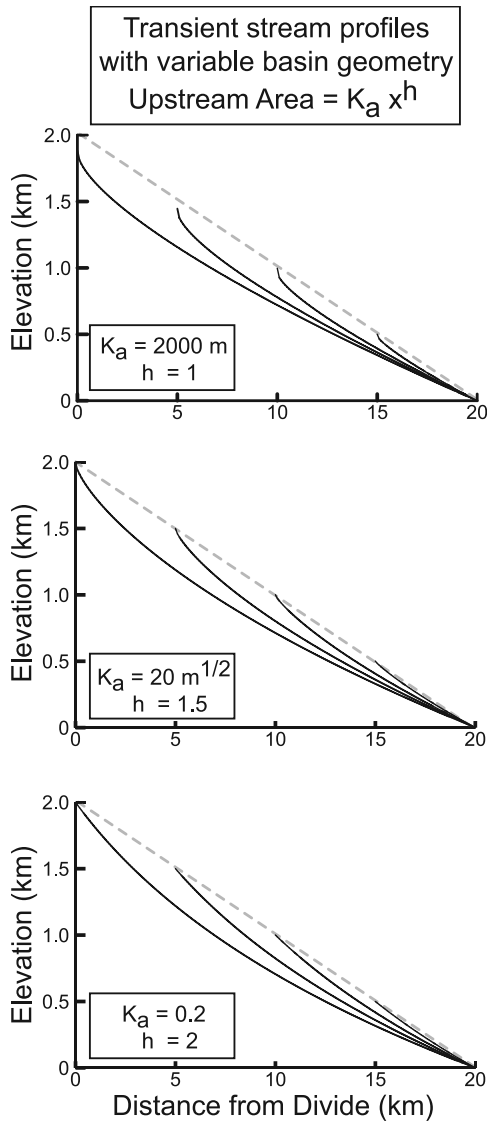


Figure 6. Comparison of transient channel profiles developed under different drainage basin geometries as expressed by the exponent, h . Timing of initial channel incision into unconformity is as in Figure 5b. K_a is adjusted to yield equal drainage areas at a distance of 10 km; the $h = 1$ case shows how a “pipe-like” catchment will erode more uniformly along its length because the effect of downstream increasing drainage area is damped out by the exponent, $\theta = 0.5$. More concave stream profiles are developed in the $h = 2$ case where stronger downstream increase in discharge is offset by less time of erosion in downstream portions of the unconformity surface that were more recently exposed. Very steep headwaters develop in the uppermost 0.5 km for $h = 1$ case. This occurs because the distance downstream is significantly less than K_a , leading to an unrealistically abrupt increase in discharge, and thus erosion rate, in the headwaters area.

must vary inversely with n values. *Whipple and Tucker* [1999] and *Snyder et al.* [2000] describe the same tradeoff for equilibrium landscapes. The form of transient stream profiles developed on progressively exposed unconformity

surfaces may be exploited to estimate the exponent $p = hn\theta$. Because h can be measured from topographic data and θ values generally do not vary significantly from ~ 0.5 [*Whipple et al.*, 1999], p may in turn be used to estimate n values.

[24] Inspection of modeled transient channel slopes developed within 1 km of the base of the exposed unconformity surface reveals patterns of initial channel slope with upstream channel area that vary systematically with n (insets in Figure 7). This phenomenon suggests that the slope of the channel, S_c , that develops upon exposure of the unconformity where upstream drainage area, A , is approximately constant may be used to calibrate n values. We can exploit this phenomenon by rearrangement of (1) for a finite positive amount of erosion, ϵ , after the onset of exposure of the unconformity surface for a span of time, Δt ,

$$\frac{\epsilon}{\Delta t} \approx K_e K_d^n (A^\theta S_c)^n. \quad (16)$$

[25] Realizing that we can interchange time for distance with the relationship, $V\Delta t = S_0\Delta x$,

$$\frac{\epsilon}{\Delta x} \approx K_e K_d^n \frac{S_0}{V} (A^\theta S_c)^n. \quad (17)$$

[26] This equation can be further rearranged by substituting the difference between channel slope and the unconformity slope,

$$\Delta S = S_0 - S_c = \frac{\epsilon}{\Delta x}, \quad (18)$$

into (17). Taking the logarithm of both sides yields

$$\log(\Delta S) \approx \log\left(\frac{S_0 K_e K_d^n}{V}\right) + n \log(A^\theta S_c), \quad (19)$$

which defines a line with slope, n . This relationship predicts that the change in slope, ΔS , will be more sensitive to drainage area with higher values of n , a result that is qualitatively consistent with both approximate analytic (Figure 7) and numerical (Figure 8) results. Slope and area data from multiple channels developed into a uniformly tilted and exposed unconformity surface may be graphed according to (19) to empirically estimate n even if the constants K_e , K_d , and V are unknown. However, the error in this analysis is very sensitive to the measured channel slope. Figure 9 shows plots derived from the average slopes for the last 100 m of channel profiles developed under different n values. Trends defined from numerically simulated channel profiles (Figure 8) are consistent with the relationship predicted by (19). Trends defined from channel profiles derived from approximate analytic model for $n < 1$ and $n > 1$ are systematically biased at larger drainage areas, resulting in erroneously low or high n values, respectively.

[27] Observation of concordant but narrow ridge lines is not sufficient evidence of a relict paleosurface. Such a pattern also arises in landscapes where erosion rates are in dynamic equilibrium with rock uplift rates (Figure 10). Equation (4) describes equilibrium channel profiles where erosion rate balances a spatially constant uplift rate, U (Figures 10a and 10b). The headwaters elevations from

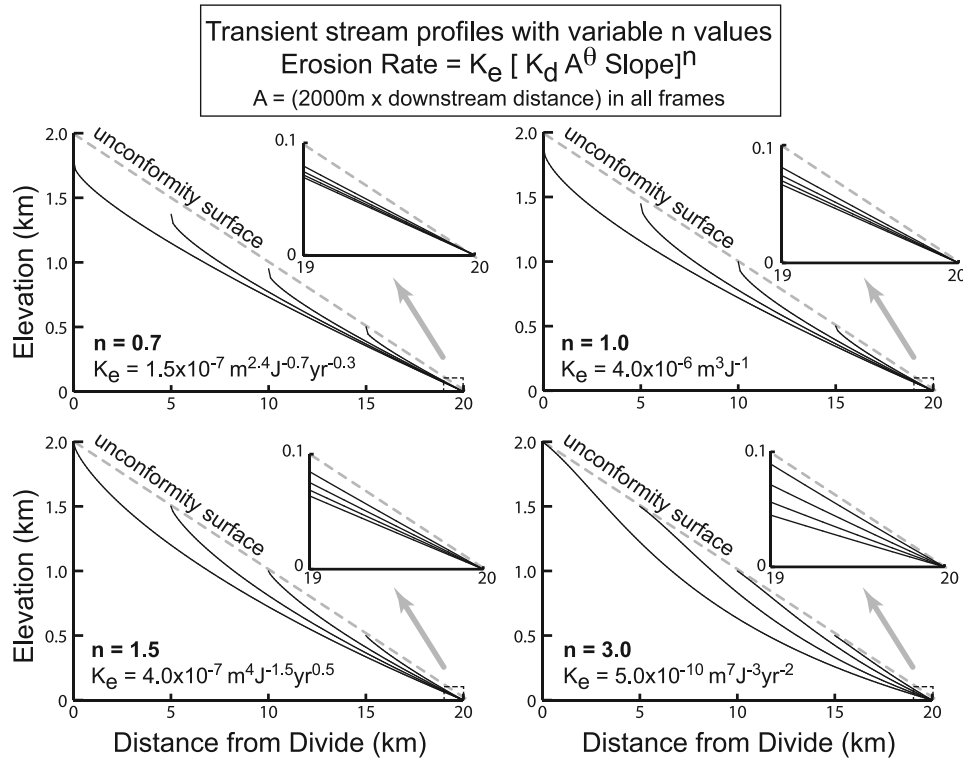


Figure 7. Transient channel profiles for “pipe-like” catchments developed under different values of n . K_e values are scaled to give approximately the same initial erosion rate at 10 km distance downstream. Values vary by over 3 orders of magnitude because units of K_e vary with n . Geometric properties $\theta = 0.5$ and $h = 1$ are the same for each model. Timing of initial channel incision into unconformity is as in Figure 5b. Here n values significantly affect the shape of transient channel forms. Insets of last kilometer of channel profiles show significant difference in the distribution of channel slopes with n .

these profiles define concave downward envelopes that do not mimic an initially planar surface unless the intrinsic concavity, θ approaches low values ($\theta \leq 0.3$). Alignment of channel headwaters elevations can be more readily obtained under equilibrium conditions with spatially variable rock uplift rate. This effect was explored by Kirby and Whipple [2001], who found that a power law distribution of uplift rates could yield channels with linear or even concave downward profiles. We illustrate a similar pattern with channel profiles at erosional equilibrium with a linear downstream trend in uplift rate,

$$U(x) = U_0 + U_1 x, \quad (20)$$

where U_0 and U_1 are constants (Figures 10c and 10d).

[28] Though certain cases of spatially variable uplift rates can result in aligned headwaters elevations in dynamic equilibrium, the resulting patterns of channel steepness or concavity contrast strongly with those of transient channel profiles developed on a progressively exposed, tilted, planar unconformity surface (e.g., Figure 5). Upstream increasing uplift rates enhance concavity of channel profiles, contrary to the low concavity of the transient channel profiles. Downstream increasing uplift rates result in very steep channels in small catchments near the toe of the slope, rather than channel slopes very near the slope of the unconformity. Though a combination of low intrinsic concavity and upstream-increasing uplift rates could produce a

distribution of equilibrium channel profiles that closely resemble the transient profiles presented here, the lag in erosion rate for tributary channels with headwaters that start at a lower position than the trunk stream should lead to ubiquitous formation of knickpoints above tributary junctions in transient landscapes (Figure 5c). Equilibrium landscapes, by definition, should not systematically develop knickpoints in this manner.

4.2. Analysis of the Kyrgyz Range

[29] Six unglaciated catchments selected from the south facing slope of the east Kyrgyz Range (Figure 2) separate concordant planar panels interpreted as the exposed pre-Cenozoic unconformity surface by Oskin and Burbank [2005]. Concordant headwaters and interfluves of these catchments define a low-relief upland surface with a slope of 0.18 (Figure 11). This relict surface is deeply incised by larger drainages that descend from the range crest (Figure 2).

[30] Inverse modeling of channel slopes at the foot of the range to calculate n values using (19) proves problematic because of noise inherent in the available Shuttle Radar Topography Mission 3 arc second data. This noise is visible as east-west striping in slopes (Figure 2) and as undulations in channel profiles (Figure 11). Channel slopes at the foot of the unconformity surface range from 0.10 to 0.13, which is significantly less than the initial unconformity slope of 0.18. The close range of initial channel slopes is consistent with n

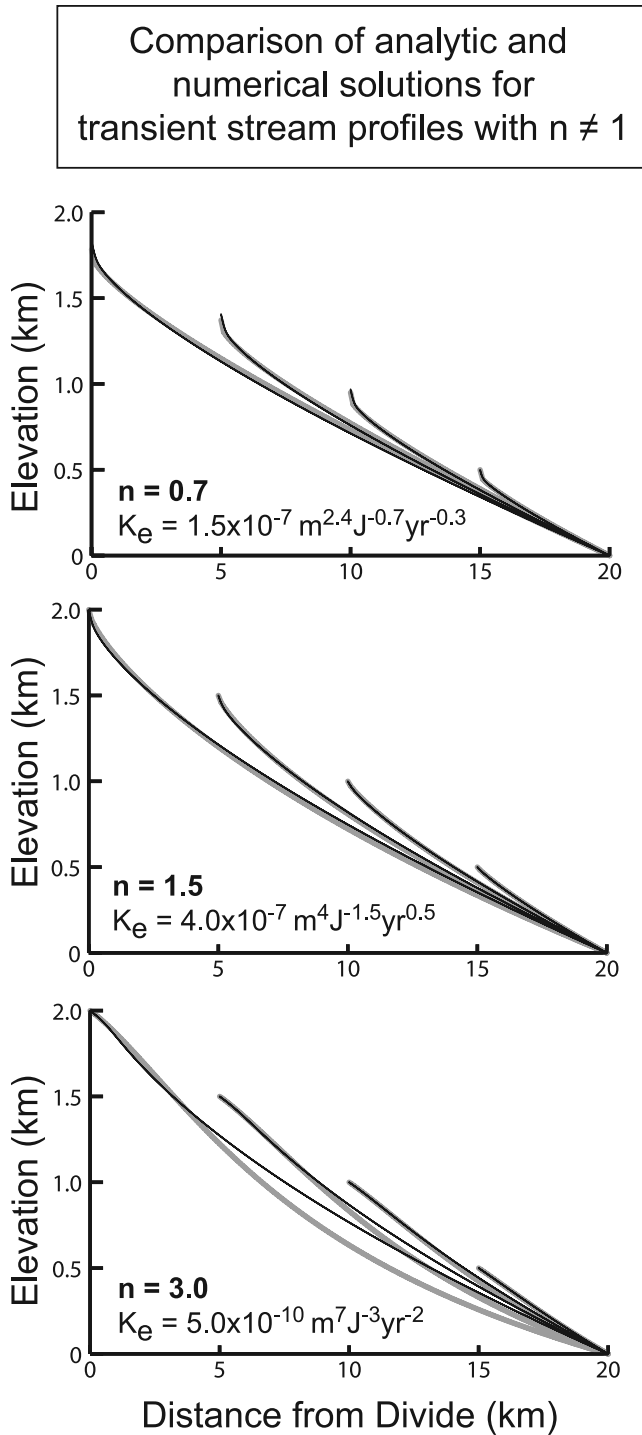


Figure 8. Numerical simulations of transient channel profiles for “pipe-like” catchments developed under different values of n compared with approximate analytical solutions. Black lines are numerical results overlain on gray lines from analytic approximations. Analytic approximations qualitatively agree well with simulations for $n = 0.7$ and $n = 1.5$ but poorly with simulation of $n = 3$ case. Headwaters node of numerical simulations is held fixed at 5 m above first simulated node at $x = 10$ m.

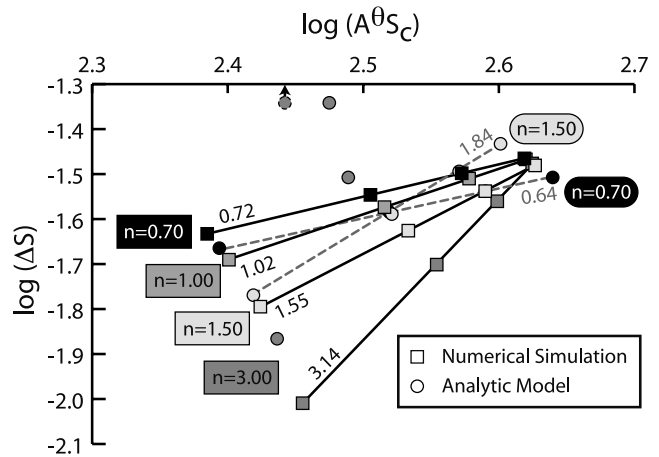


Figure 9. Plots of $\log(\Delta S)$ versus $\log(A^\theta S_c)$ for last 100 m of analytic models (circles and gray dashed lines) and numerical simulations (squares and black solid lines) of transient channel profiles developed on a progressively exhumed unconformity. These profiles are identical for the $n = 1$ case. These points define lines with slope (shown as numbers next to each line) that may be used to estimate n . Slope values derived from numerical simulations predict n within 5%. Linear trends derived from analytic models for $n = 0.7$ and $n = 1.5$ show systematic bias as a result of substitution of initial slope, S_0 for channel slope, dz/dx in (7). Points from poorly fitting $n = 3$ analytic model do not define a linear trend.

values near 1 but is not of sufficient quality to further quantify n . Higher-quality topographic data and field measurements may improve the results of this method by reduction of slope errors and expansion the range of catchment sizes analyzed.

[31] Catchments developed on the south facing slope of the east Kyrgyz Range are geometrically similar, with $h = 1.4 \pm 0.1$, permitting comparison to a single set of solutions (e.g., Figure 6). Forward modeling of channel profiles (Figure 11) proves sensitive to the chosen value of n . Solutions with $n \leq 1$ overestimate the concavity of the upstream portions of the larger channels, while solutions with n as high as 1.5 underestimate the concavity of these same reaches. A best fit solution was obtained with $n = 1.2$, and the fit improved with a slight reduction of the intrinsic concavity, θ , to 0.45.

[32] One important caveat to the forward modeling approach is that, because of events such as drainage capture, observed channel profiles may have developed under different conditions, such as a larger or smaller catchment area, than those seen at present. The stream profiles in Figure 11 follow the longest pathways presently available in each catchment. However, stream capture events may shorten a catchment and result in a truncated or distorted channel profile. For example, the low-gradient trunk stream of catchment 1 abruptly ends and appears to have been beheaded (Figure 2). Near the point where the trunk stream of catchment 1 was beheaded, the longest available pathway follows a steep tributary stream, resulting in an abrupt steepening of the channel profile on Figure 11. A capture

Equilibrium stream profiles with concordant, quasi-planar interfluves
 $h = 1, n = 1$ in all frames

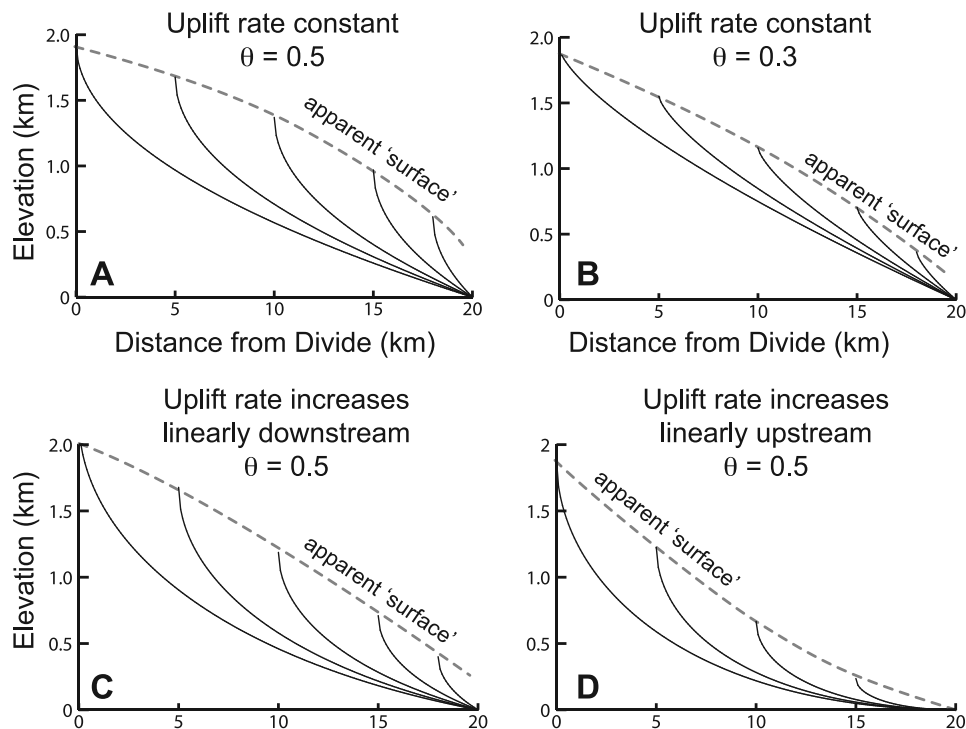


Figure 10. Channel profiles at equilibrium with rock uplift rates. Gradients in uplift rate and low intrinsic concavity can align headwater elevations to yield an apparent relict surface in the landscape. However, the distribution of channel shapes, especially near the headwaters, differs from transient cases.

event may also explain an apparent truncation of the end of catchment 4.

[33] It is also important to keep in mind that stream power is a simplified model for bedrock channel erosion, and thus

the n values calculated here are limited by the assumption that this model can describe erosion along the lengths of these channels. Transition from debris flow dominated to fluvially dominated erosion [Stock and Dietrich, 2003],

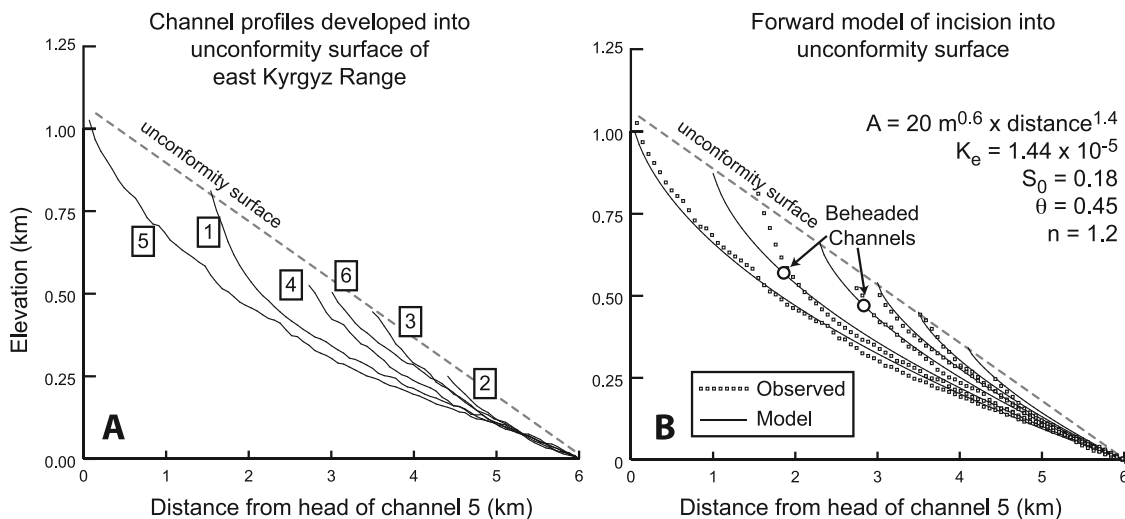


Figure 11. (a) Channel profiles extracted from the SRTM topography for catchments 1 through 6 on south facing slope of east Kyrgyz Range. See Figure 2 for channel locations. (b) Forward model of channel incision into unconformity surface with channel elevation data shown as points. Significant diversions from the model occur where channels appear to have been beheaded via stream capture.

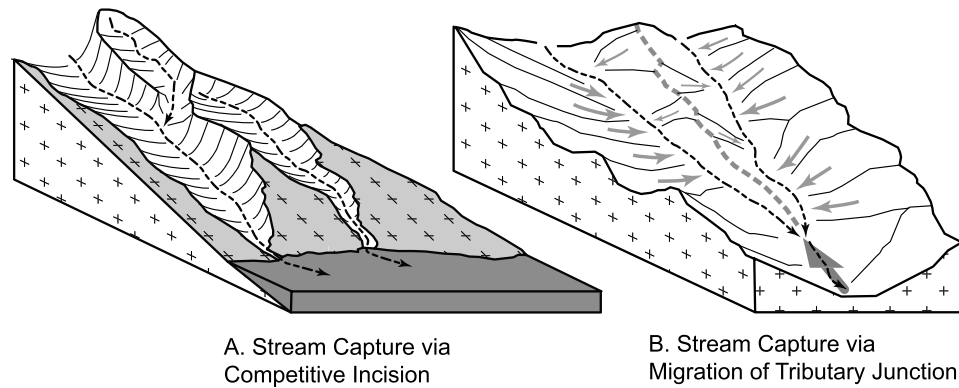


Figure 12. Two potential mechanisms of stream capture in transient landscape evolution of the Kyrgyz Range. (a) Capture via competitive fluvial incision and undermining of adjacent catchment. (b) Capture via upstream migration of tributary junction. We speculate that slow removal of interfluvium by lateral channel incision may be driven by asymmetric flux of debris from tributary channels.

downstream variations in the availability of bed load to abrade the channel [Sklar and Dietrich, 1998, 2004; Wobus *et al.*, 2006], and transition to transport-limited conditions [Lavé and Avouac, 2001] all may affect the shape of a channel profile. Thus the value of n derived from shapes of channel profiles may not reflect the local dependence of bedrock erosion rate on stream power. Further insights into the local dependency of n could be gained from studies that combine the inverse- and forward-modeling approaches with field observations of channel slopes and bed load cover.

5. Competitive Fluvial Incision

[34] As drainage basins lengthen and widen, drainage capture must be an ubiquitous process [Ellis *et al.*, 1999; Densmore *et al.*, 2004, 2005; Ijjasz-Vasquez *et al.*, 1993]. This most likely is accomplished by “stream piracy” whereby portions of adjacent, smaller catchments are rerouted into larger catchments (Figure 12a). For the case of a progressively exposed unconformity surface described in the previous section, these capture events do not readily occur at the foot of the exhumed unconformity surface because adjacent stream outlets are often distant from each other and lengthen directly downslope as the unconformity is progressively exposed. However, as incision of channels with larger catchment areas outpaces incision of channels with smaller catchment areas, upstream portions of the smaller catchments are undermined, resulting in tributaries that essentially “fall off” into the larger catchment, leaving behind a beheaded channel in the smaller catchment (Figure 12a). This is similar to the capture process observed in numerical models of optimal channel network development [Ijjasz-Vasquez *et al.*, 1993]. Another, more subtle capture process may occur through the migration of tributary junctions (Figure 12b). The drainage configuration that results from either type of capture event may not be stable because channels with larger upstream catchment areas, and thus greater stream power at a given channel slope, will progressively undermine and capture drainage area from adjacent catchments and tributaries. Thus competitive fluvial incision can drive

further stream piracy as well as reorganization of tributaries within a catchment.

5.1. Analytic Model of Competitive Fluvial Incision

[35] A model for competitive fluvial incision of two adjacent catchments (Figure 13) illustrates the positive feedback system that drives further drainage reorganization. We consider a simple system of two parallel, “pipe-like” catchments with erosion rate that everywhere balances rock

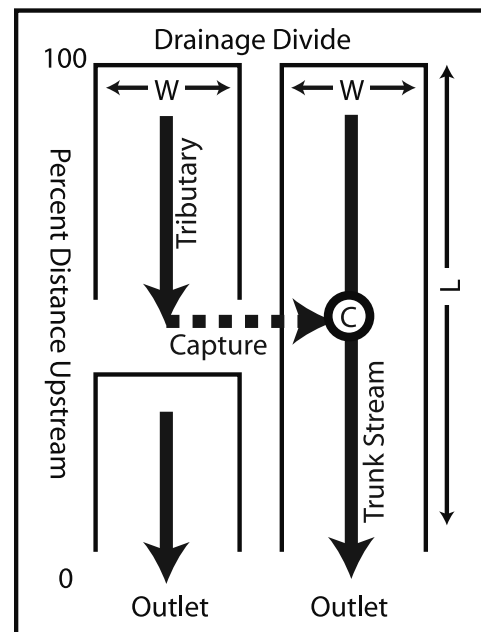


Figure 13. Schematic model of two adjacent catchments of length, L , and width, W , with stream capture at point C . All streams are modeled at erosional equilibrium with rock uplift. The benefit of stream capture is measured by the elevation at the headwaters which integrates channel slope over L : Lowest headwater elevation correlates with greatest benefit. Model presented here does not predict the location of the capture point, C , but only the effect should a capture take place.

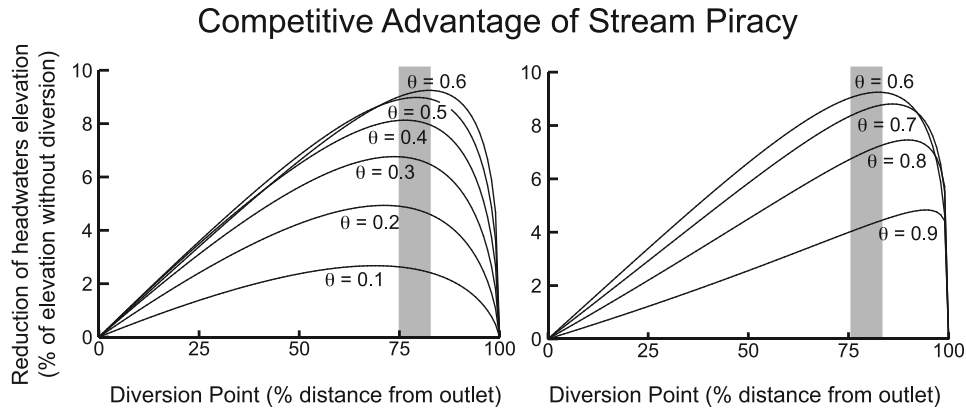


Figure 14. Graphs of equation (22) showing maximum benefit of stream piracy dependent upon the location of the capture point. Gray band shows zone of maximum benefit for commonly measured values of θ . In this band, the optimal capture point position lies approximately 75–85% upstream of the outlet. Graphs are split for clarity at $\theta = 0.6$.

uplift according to (4). Because this model compares equilibrium channel profiles, it is most analogous to the hypothetical migration of tributary junctions shown in Figure 12b. A capture point, C , is placed between two adjacent catchments of width, W , and length, L . Drainage area, A , is defined (Figure 13) as a function of distance upstream, x and the position of C between the two basins,

$$A = W(L - x), \quad x > C \quad (21)$$

$$A = W(2L - C - x), \quad x \leq C. \quad (22)$$

[36] Disregarding the distance between the two catchments, integration of (3) by parts in the upstream direction yields the headwaters elevation,

$$z(L) = \left(\frac{U}{K_e}\right)^{\frac{1}{n}} \frac{1}{K_d W^\theta (1 - \theta)} \times \left[(L - C)^{1-\theta} + (2L - C)^{1-\theta} - (2L - 2C)^{1-\theta} \right]. \quad (23)$$

[37] Competitive advantage varies by the position of the capture point within the schematic pair of basins (Figure 14). Though expressed as the relative difference in elevation at the headwaters, this difference arises from the addition of discharge below point C and affects the entire channel elevation above the outlet. Where $C = 0$, the two catchments are independent of one another and thus there is no advantage gained. Where $C = L$ no advantage is gained because no upstream drainage area exists above the capture point. For every capture point between 0 and L , some competitive advantage exists for stream capture for $0 < \theta < 1$ (Figure 14). The maximum advantage occurs where the capture point lies closer to the headwaters than the outlet, with position and maxima that depends upon θ . For the commonly observed range of θ values for bedrock channels, from 0.35 to 0.6 [Whipple *et al.*, 1999], advantage gained approaches the maximum value of about 10 percent. This amounts to 200 to 300 m of differential incision at the scale

of fluvial relief present in the north facing slope of the Kyrgyz Range (Figure 1).

[38] It is useful to consider the transient response of channel network to a drainage capture event (Figure 15). Immediately after a capture event, before channel slopes have adjusted, the channel incision rate, E , downstream of the capture point, C , increases by the ratio,

$$\frac{E_{(x \leq C)}}{E_{(x > C)}} = \frac{-K_e A_{(x \leq C)}^\theta \left| \frac{dz}{dx} \right|^n}{-K_e A_{(x > C)}^\theta \left| \frac{dz}{dx} \right|^n}. \quad (24)$$

[39] The erodibility constant, K_e and the initial slope, $\frac{dz}{dx}$, cancel out. The ratio of catchment areas determines the ratio of erosion rates,

$$\frac{E_{(x \leq C)}}{E_{(x > C)}} = \left[\frac{W(2L - 2C)}{W(L - C)} \right]^{n\theta} = 2^{n\theta}. \quad (25)$$

[40] After the capture event, the slope of downstream portion of the channel profile will relax as it adjusts to the new, more erosive condition [Whipple and Tucker, 1999]. Simultaneously a wave of incision will propagate upstream

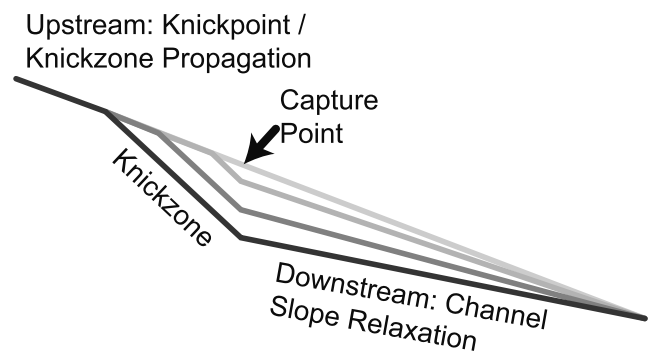


Figure 15. Response of an equilibrium channel to a capture event at point C . Downstream reach increases incision rate and relaxes to a lower slope. Upstream reach sees a growing wave of incision as a knickzone propagates upstream.

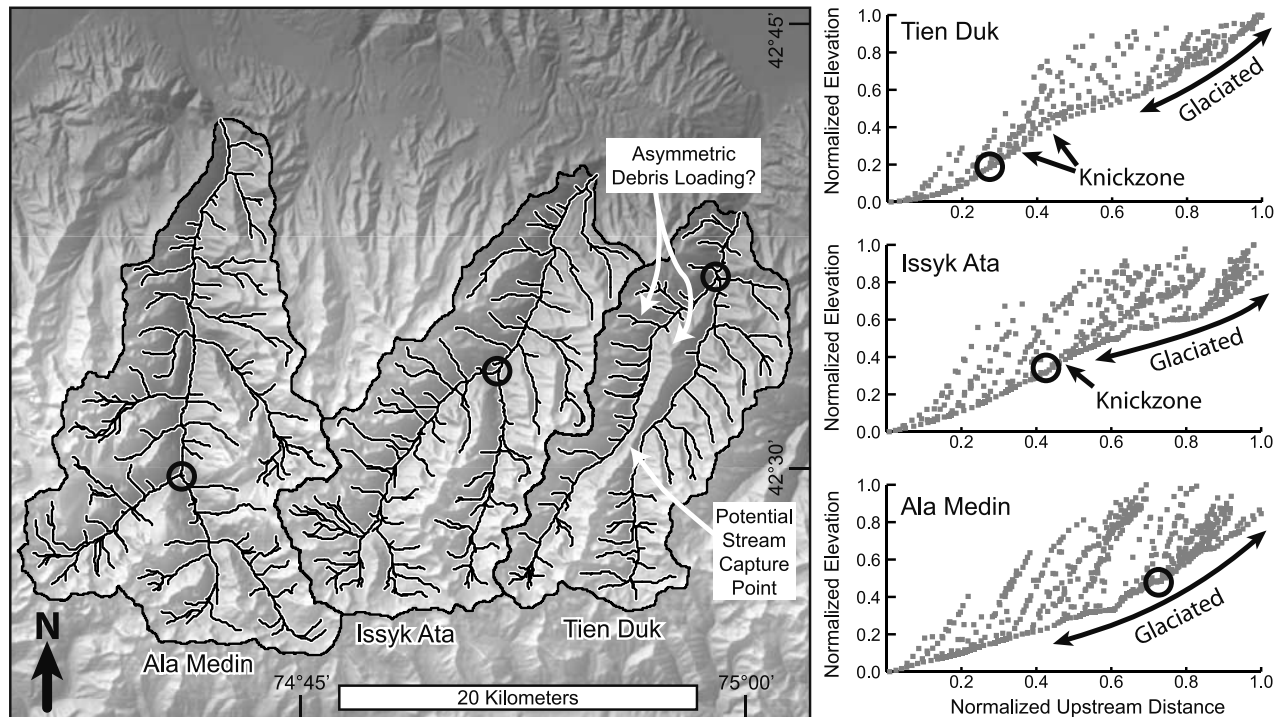


Figure 16. Map of three catchments at boundary of transition zone and steady morphology zone of the central Kyrgyz Range showing the catchment-scale effects of the positions of tributary junctions. Note that the position where tributaries join to form a single trunk stream channel (open circles) varies from near the range front to well into the range interior. Graphs of channel segment elevations versus distance from the range front, normalized for elevation and catchment length, indicate greater relative incision for catchments where the trunk stream penetrates deeper into the range. Knickzones are broad convexities developed upstream of tributary-trunk junctions and well downstream of glacially eroded reaches, indicating a possible transient effect of recent stream capture or upstream migration of the tributary junction point. Abrupt steepening of Ala Medin trunk stream downstream of the tributary junction point is a result of an artifact present in the topography data.

from the capture point. Because erosion of the downstream side will deepen the knickpoint over time, the wave of incision will spread out as a knickzone of increased channel steepness upstream of the capture point (Figure 15).

[41] The competitive incision model presented here does not consider the cause of a capture event, only the result of such an event on the eventual amount of fluvial relief. For the idealized model setup shown in Figure 13 we would expect these adjacent channels of equal size to incise at equal rates. This configuration is metastable [Ijjasz-Vasquez *et al.*, 1993]. In a more realistic situation, adjacent catchments will not be equally sized, and larger catchments will progressively undermine and capture the smaller ones [Ellis *et al.*, 1999; Densmore *et al.*, 2005]. The transient wave of incision following one capture event can promote further capture events upstream because the knickpoint wave speed is proportional to the upstream drainage area (represented as upstream distance, x , in (6)). Thus a wave of incision will move faster up the larger catchment, giving it additional advantage to undermine upstream portions of the smaller catchment.

5.2. Analysis of the Kyrgyz Range

[42] Comparison of three adjacent catchments developed on the deeply incised north facing slope of the Kyrgyz

Range (Figure 16) provides a field example of the effect of drainage capture on channel profiles and possible examples of the migration of junction points idealized in Figures 12 and 15. Stream profiles, scaled by length, reveal that presteady state Tien-Duk and Issyk Ata catchments are not as deeply incised as the Ala Medin catchment, which lies in the steady morphology zone of the Kyrgyz Range (Figures 16 and 1). The less incised canyons of the Tien Duk and Issyk Ata rivers have major tributary junctions that lie well downstream of the optimum position predicted by the graphs in Figure 14. Convexities occur just upstream of these tributary junctions and downstream of the extent of glaciation. These convexities are consistent with a wave of incision upstream of a recent capture point or with tributary junction points that are migrating upstream. Note that this evidence does not substantiate that migration of tributary junctions is occurring here. Other processes, such as a knickpoint propagating upstream from the range front, could also form the observed convexities. A probable future capture point is predicted for the Tien Duk river where two tributaries, separated by 200 m elevation, approach within 1 km (Figure 16). If this capture occurs, a wave of incision would move upstream from this point while the abandoned downstream portion of the tributary valley is undermined by the more rapidly incising trunk stream.

Kyrgyz Range Drainage Basin Geometry

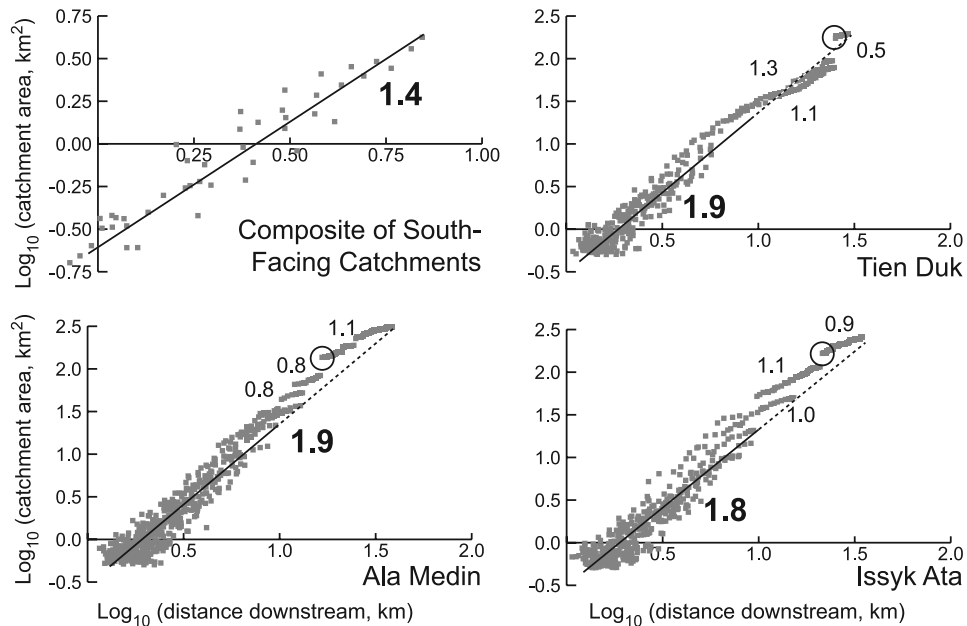


Figure 17. Analysis of downstream distance versus drainage area for catchments on the south and north facing slopes of the Kyrgyz Range. South facing catchments are from Figure 2; Ala Medin, Issyk Ata, and Tien Duk catchments are from Figure 16. Point clouds in lower-left corner of each graph represent small catchment, low-order tributaries. Note different scale of the south facing catchments graph. Regression slopes, corresponding to values of h in $A = K_d x^h$, of lower-order channels with drainage areas $<20 \text{ km}^2$ are shown by lines and bold numbers. Dashed lines show extrapolation of these trends to larger catchment areas. High-order tributary and trunk streams define distinct segments with lower h values, shown as numbers next to aligned points. Major tributary junctions correlate to the largest steps between segments, with upstream end of trunk streams outlined by the open circles.

[43] Though the idealized capture model shown in Figure 13 cannot be directly applied to the examples described here, the general effect of stream capture and progressive widening of drainage basins is revealed by the relative organization river networks developed on the unconformity surface (Figure 2) and in the transition zone (Figure 16). The positive feedback between drainage capture and deepening of channel incision drives transformation of catchments from “pipe-like” ($h = 1$) to “box-like” forms ($h = 2$). The “box-like” end-member, found by *Montgomery and Dietrich* [1992] to be the general case over 13 orders of magnitude of drainage basin sizes worldwide, probably represents the maximum rate of gain of drainage area versus channel length on a two-dimensional surface. We developed an analysis similar to that of *Montgomery and Dietrich* [1992] but confined to individual catchments or sets of catchments (Figure 17). Channel segments between 500 and 1000 m in length were extracted from the digital elevation data, and the catchment area and maximum upstream distance to the divide were calculated for each segment. The slope of catchment area versus distance, plotted in log-log space, yields the length-area scaling, h , for the inverse of Hack’s Law (equation (2)). This analysis illustrates that “box-like” catchments in the Kyrgyz Range develop through the elaboration of tributary stream networks. Nascent catchments incising the south facing slope have a low value of $h = 1.4 \pm 0.1$. Conversely, tributaries with drainage

areas $<20 \text{ km}^2$ in the much larger and deeper-incised catchments on north slope of the Kyrgyz Range define trends approaching $h \approx 2$. The collected points from the larger tributaries and trunk streams fall near the trends defined by the smaller tributaries. However, individual reaches with the largest drainage areas ($>10 \text{ km}$ downstream; see Figure 17) define discrete sets of points with noticeably lower values of $h \approx 1$. The segments with the largest drainage areas are more continuous within the Tien Duk and Issyk Ata catchments than within the Ala Medin catchment, where the segments are interrupted more frequently by junctions with large tributaries. The overarching effects of formation and (re)distribution of major tributary junctions is to fragment the largest streams and increase their catchment area in a more stepwise fashion downstream. These effects in turn drive the overall length-area scaling of the catchment toward a more “box-like,” $h = 2$ trend.

[44] The tendency toward development of $h \approx 2$ scaling of catchment area with distance, (Figure 17) and the resultant deepening of channel incision toward the central, steady state portion of the range (Figure 16) are critical to attaining balance between erosion rate and rock uplift rate without building excessive fluvial relief. Figure 18 shows two sets of 40-km-long equilibrium channel profiles modeled with 1 mm/yr rock uplift rate, consistent with exhumation rates in the central portion of the range from *Sobel et al.* [2006]. K_e , θ , and n values were obtained from forward

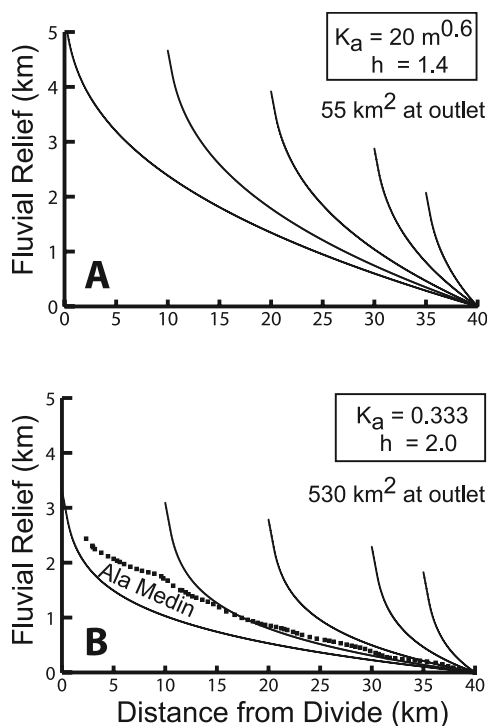


Figure 18. Channel profiles at erosional equilibrium with uniform rock uplift rate of 1 mm/yr and rock erodibility, K_e , and n values calibrated from transient channel profiles on south facing slope of the Kyrgyz Range. (a) Channel profiles with area-length relationship as on south facing slope, with $h = 1.4$, which require 5 km of relief over 40 km distance for incision to balance rock uplift rates. (b) Channel profiles with area-length scaling $h = 2$ [Montgomery and Dietrich, 1992], similar to that observed from large drainage basins of central Kyrgyz Range, requiring only 3 km of relief over 40 km distance to balance rock uplift rates. Points from Ala Medin River are plotted for comparison. Note that catchment area at outlet for 40-km-long streams differs by an order of magnitude between $h = 1.4$ and $h = 2$ cases.

modeling transient channel profile development on the south facing slope (Figure 11). The 40-km channel length is similar to the channel lengths of the largest catchments developed in the central portion of the Kyrgyz Range. Using $K_a = 20 \text{ m}^{0.6}$ and $h = 1.4$, consistent with the channel networks developed on unconformity surface, yields 5000 m of fluvial relief (Figure 18a). If instead the area-length scaling is changed to $K_a = 0.333$ and $h = 2$ from Montgomery and Dietrich [1992], comparable to the observed area-length scaling in the steady state portion of the Kyrgyz Range (Figure 17); then only 3000 m of relief is gained along 40 km of channel length (Figure 18b). The stream profile of the ~40-km-long, 415 km² Ala Medin catchment is overall slightly steeper than the equivalent fluvial model except at its glaciated headwaters, which is less steep than expected. This same pattern has been observed in other glaciated landscapes [Brocklehurst and Whipple, 2002], and could suggest that transient adjustment of the channel profile is ongoing at this position within the Kyrgyz Range. However, glaciation, and the effects of till on downstream

portions of the fluvial system, have not been included in the simple model developed here.

6. Discussion

6.1. Basement-Cored Surface Uplift

[45] Systematic changes in channel profiles and channel network geometries accompany surface uplift and relief production in the Kyrgyz Range. Upon exposure of resistant basement rocks as readily eroded Cenozoic strata are stripped off the growing range, surface uplift dominates as channels gradually incise and develop progressively more concave profiles over time. The modeling results presented here support the contention that headwaters and interfluvial regions can persist at or near the elevation of an exhumed unconformity surface as channels simultaneously lengthen and incise into progressively exposed, erosionally resistant basement. Because of the close relationship of channel form to the time of exposure of resistant bedrock, the imprint of the unconformity surface can persist on the landscape as an interpretable relict landform over a length scale comparable to the width of the range. The headwaters and interfluvial regions define a concordant upland “surface” that closely mimics the former position of the unconformity, as is commonly observed in the Tian Shan and other basement-involved orogens [Davis, 1904; Burbank *et al.*, 1999; Abdрахmatov *et al.*, 2001; Jordan and Allmendinger, 1986; Gregory and Chase, 1994; Spotila *et al.*, 1998]. Our modeling further indicates that knickpoints should develop at tributary junctions because of persistent disparities between erosion rates of tributary and trunk streams. This phenomenon provides an important quantitative test of the hypothesis that a concordant upland region results from a transient response to surface uplift and is not a misinterpretation of an equilibrium landscape (Figure 10).

[46] Though building of topography with exposure of resistant basement rocks is an intuitively expected result, predicting the amount of surface uplift that should result is not as straightforward because rock uplift, U , or the unconformity exposure rate V , are not directly comparable to erodibility, K_e . Eroding must be transformed into an erosion rate via the catchment area and slope of a river via (1). These erosion rates will vary spatially as channel networks develop on the exposed basement rocks. Under the conditions of a progressively exposed basement-cored block, where the tilt of the basement cover unconformity sets the initial channel gradient, equilibrium conditions between rock uplift rate and river incision rate, if ever achieved, will likely first occur at the foot of the range where river catchment areas are greatest. Once achieved, equilibrium channel slopes will gradually replace upstream portions of the drainage network at a vertical rate comparable to the rock uplift rate [Wobus *et al.*, 2006]. Equilibrium may also be achieved first in the headwaters as channel slopes progressively steepen because discharge, and thus erosion rate, increase downstream (Figure 5). Thus the middle portions of these transient channels, where there is the greatest difference between the initial unconformity position and a final, equilibrium stream position, are likely to be the last part of the landscape to fully adjust.

[47] Processes that control the position of the divide at the range crest (z_0 in Figure 4) also control the conditions for

whether equilibrium can be achieved in catchments incised into the unconformity surface. So long as the divide is moving upward and away from the foot of the range, equilibrium is only gradually approached as steepening slopes develop in the headwaters (Figure 5a). If instead the divide position becomes fixed with respect to the foot of the range where the unconformity surface is first exhumed, then there are two potential outcomes so long as the rate of exposure of the unconformity, V , remains constant. (1) If catchments are large enough to achieve equilibrium between incision rate and the rate of exposure of bedrock at the foot of the range, equilibrium channel gradients will be established and this equilibrium state will propagate upward through the channel network. (2) If catchments are too small to establish equilibrium, transient conditions will persist as rocks are advected through the landscape. Numerical models of landscape evolution on the backlimbs of fault bend folds arrive at a similar result [van der Beek *et al.*, 2002; Miller *et al.*, 2002]. For the case of the Kyrgyz Range, remnants of the unconformity surface persist to the topographic divide near 4000 m elevation where glacial erosion incises both north and south facing headwater reaches [Oskin and Burbank, 2005]. The approximately 1500 m of relief traversed by the channels incised into the 10- to 15-km-long south facing slope is insufficient to have developed equilibrium channel relief (2000 to 3000 m, Figure 18a). Thus in this setting surface uplift appears limited by glacial erosion [Oskin and Burbank, 2005] before equilibrium fluvial channels can be established. In other settings, steeper fluvial channels developed on the opposing range slope or cross-range differences in base level may ultimately set range height [Densmore *et al.*, 2004, 2005; Ellis and Densmore, 2006].

6.2. Transition to Steady State

[48] In contrast to the southern flank of the Kyrgyz Range where the unconformity surface is being progressively exhumed, development of large, deeply incised catchments on the northern flank of the Kyrgyz Range ultimately tend toward a balance between rock uplift and erosion in the central portion of the range where significant exhumation of reset thermochronometers has occurred [Sobel *et al.*, 2006; Bullen *et al.*, 2001]. Achieving this balance is aided by development of “box-like” drainage networks where area-length scaling, $h \approx 2$, maximizes downstream increase of discharge with distance (Figure 18b). Drainage capture processes, including possibly the migration of tributary junctions, incrementally increase net stream power expended on the trunk streams, resulting in greater rates of channel incision and deepening of catchments (Figures 14 and 16). Thus the rates of capture processes are one of the key arbiters as to whether a basement-cored rock uplift can be balanced by erosion. Though this study does not directly address these rates, we have observed two processes in the field that could prove important for setting catchment expansion rates: (1) undermining of upstream portions of tributaries, as observed for both south facing catchments (Figure 2) and north facing catchments (Figure 16), and (2) asymmetric debris loading from lower-order tributaries (Figure 12b). Undermining of upstream portions of tributaries will occur in proportion to the relative rates of knickpoint propagation

for the trunk and tributary streams (Figure 15) but is limited by the relative depth of incision and the height of intervening hillslopes. Asymmetric debris loading is a previously undocumented process that we propose to occur where a narrow septum-like ridge exists between two large tributaries. The sediment flux from low-order tributaries on the septum is less than that from the larger low-order tributaries emerging from the opposite valley side. Because a small proportion of debris from these tributaries will tend to reside temporarily at tributary junctions [Benda and Dunne, 1997], the asymmetry of debris production will tend to drive the active stream channel toward the septum and promote lateral incision (see Figure 16), further narrowing of the interfluvium, and driving upstream migration of the tributary junction or a drainage capture event.

[49] Additional unmodeled effects of tilting and glaciation have affected landscape evolution of the Kyrgyz Range. The dip of the unconformity surface preserved on the south facing slope of the eastern Kyrgyz Range gradually steepens from east to west, probably in response to a gradient of slip on a curvilinear reverse fault at depth [Abdrakhmatov *et al.*, 2001; Oskin and Burbank, 2005; Sobel *et al.*, 2006]. If the fault is curvilinear then the unconformity must progressively tilt during shortening [Amos *et al.*, 2007]. Tilting enhances erosion rates in all channel profiles simultaneously and does not yield the systematic deepening of profiles away from the foot of the range predicted from progressive exposure of the unconformity. Thus, although tilting is likely to have occurred during surface uplift, further invigorating channel incision, the overall pattern of channel development remains consistent with the model of progressive exposure of a planar surface of resistant basement. Glaciation plays a pivotal role in the transition from steep catchments with shallowly incised transient channels developed in the surface uplift zone to large catchments with deeply incised channels in the steady morphology zone of the Kyrgyz Range [Sobel *et al.*, 2006]. Foremost, glacial erosion appears to effectively limit peak elevations near the equilibrium line altitude [Oskin and Burbank, 2005], consistent with the “glacial buzz saw hypothesis” of Brozovic *et al.* [1997]. Other effects of glaciation via changes to basin hydrology [Aizen *et al.*, 1995], periodic glacial erosion [Anderson *et al.*, 2006], and pulsed glaciogenic sediment production [Church and Ryder, 1972] require further attention to complete understanding of landscape evolution in the Kyrgyz Range.

[50] Ultimately, the response time for formation of large, integrated drainage networks with erosion rates sufficient to balance rock uplift rates determines whether the threshold is crossed for propagation of faulting into the foreland [Hilley *et al.*, 2005]. Thus far we have considered whether surface processes can establish sufficient erosion rates. Alternatively, as a limiting elevation is approached, rock uplift rates may instead diminish as tectonic shortening migrates elsewhere [Molnar and Lyon-Caen, 1988]. Such an effect does not appear to have substantially slowed exhumation of the central Kyrgyz Range where a (U-Th)/He cooling ages as young as 3 Ma support sustained exhumation of at least 0.8 mm/yr since the late Pliocene [Bullen *et al.*, 2001]. However, an interplay between limited erosion of basement and distribution of shortening rates may generally drive the distributed fault activity observed in active belts of base-

ment-cored uplifts [*Jordan and Allmendinger, 1986; Thompson et al., 2002*].

6.3. Broader Implications

[51] Though formulated to investigate the topographic response to surface uplift of a resistant basement block, the relationships developed in this paper have broader potential applications for understanding transient landscape evolution and for calibrating the stream power law from such settings. Transient channel profiles on a progressively exhumed, planar contact with a resistant lithology are a general feature of landscapes intuitively recognizable from the scale of dip slopes to orogens. We provide a quantitative test of this intuition by predicting channel form and the generation of knickpoints at tributary junctions. These tests establish a firmer basis for reconstructing landscape evolution from relict surfaces preserved in landscapes. For example, the geometry of the exhumed unconformity surface at the crest of the Kyrgyz Range was exploited by *Oskin and Burbank [2005]* to calibrate relative rates of glacial incision and cirque retreat. The generation of knickpoints in transient landscapes through stream capture and differential incision rates may also provide a basis for further investigation of stream capture as a rate-limiting process in the development of fluvially dominated landscapes where erosion rates balance rock uplift rates. The quantitative basis presented here for preservation of relict surfaces in landscapes confirms sensitivity of the transient channel profiles to the exponent, n , in (1), a value that can be related directly to the bedrock channel erosion process [*Hancock et al., 1998; Tucker and Whipple, 2002*] and stochastic effects of flood frequency [*Snyder et al., 2003; Lague et al., 2005*]. For the particular but widespread case of a progressively exposed planar contact or unconformity, this sensitivity can be exploited to simultaneously calibrate n and K_e from comparison of channels with different catchment areas but the same history defined by the exposure (or base level lowering) rate. This approach is also valid for calibrating n values even if the exposure rate is unknown, and is more flexible than calibrating n from equilibrium channel profiles where the dependence on n must be extracted from comparison of channels developed under different rock uplift rates [*Whipple and Tucker, 1999; Snyder et al., 2000*]. Measurements of channels developed into progressively exposed resistant lithologies that utilize higher-resolution topographic data sets may present a feasible approach for field calibration of n values.

7. Conclusions

[52] Basement-cored rock uplifts, commonly developed on the periphery of orogens [*Rodgers, 1987*], represent an important natural laboratory for calibrating the delicate balance between tectonic processes and erosion [*Molnar and Lyon-Caen, 1988; Sobel et al., 2003; Hilley et al., 2005*]. Using stream power modeling, we quantitatively analyze the development of river channels and the effects of stream capture processes during transient landscape evolution of basement-cored rock uplifts. This modeling is guided by observations of the Kyrgyz Range, a natural example of an active basement-cored range within the Tian Shan orogen [*Sobel et al., 2006*]. First, we examined

landscape evolution on a progressively exhumed unconformity that separates resistant basement from more erodible cover strata. We find a pattern of channel incision that characterizes this landscape. Our analysis confirms that channel headwaters and interfluves will closely mimic the initial unconformity position, reinforcing the utility of such landscapes to reconstruct channel incision and deformation [*Burbank et al., 1999*]. We also find that, although trunk-stream channels are constantly evolving and transient landforms, they take on concave profiles that may appear graded (i.e., at equilibrium) but gradually change over time. Conversely, disparate erosion rates of tributary and trunk streams leads to generation of knickpoints on tributaries upstream of their junction with the trunk stream. The existence of these features provides an important test of whether a landscape preserves evidence of a progressively exhumed relict surface. Second, we examined the role of stream capture processes in elaboration and deepening incision of channel networks. A simple model of competitive fluvial incision shows how stream capture, and possibly the migration of tributary junctions, increases expenditure of stream power on the trunk stream, promoting greater incision and a positive feedback that promotes additional stream capture. Field evidence for stream capture includes relict, abandoned downstream portions of tributary valleys and contrasting channel responses upstream and downstream of capture points. Channel gradients should relax downstream of a capture because of increased stream power, while a knickzone will gradually form and expand upstream of a capture.

[53] Balance between rock uplift and erosion rates in a basement-cored range appears to be difficult to achieve via progressive exposure of basement at the surface, as attested by preservation of unconformity surfaces up to the range crest in the Kyrgyz Range [*Oskin and Burbank, 2005*] and in other, similar settings [*Abdrakhmatov et al., 2001; Burbank et al., 1999; Jordan and Allmendinger, 1986*]. Successful balance between rock uplift rate and erosion rate in the central Kyrgyz Range [*Sobel et al., 2006*] is achieved through development of large, deeply incised and elaborated (“box-like”) drainage networks on the north facing range slope, on the opposite flank to the exhumed unconformity surface. The development of these catchments may be limited by the rates of competitive fluvial incision and stream capture, warranting further investigation of these processes.

[54] The analysis developed here, though approximate for cases where river erosion rate is nonlinearly related to slope, lends new insight into the utility of transient landscapes for calibrating surface processes. By providing a test for preservation of relict surfaces, our analysis provides a firmer basis for using these surfaces to calibrate incision rates and landscape features developed from fluvial and glacial erosion. The predictability of knickpoint formation at tributary junctions on progressively exposed unconformity surfaces also provides a new laboratory for exploring knickpoint propagation and its implications for the stream power erosion rule [*Tucker and Whipple, 2002; Crosby and Whipple, 2006*]. Similarly, the systematic response of channel incision to an imposed, steadily exposed unconformity surface slope provides a new approach for extracting mechanically important parameters of erodibility, K_e , and

the slope dependence, n , of the stream power bedrock erosion rule.

[55] **Acknowledgments.** This research was supported by NASA Shuttle Radar Topography Mission science program grant NAG5-13758. We thank K. Frankel, R. Burgette, and Associate Editor K. Whipple for reviews that substantially improved the content and clarity of the manuscript.

References

- Abdrakmatov, K. Y., et al. (1996), Relatively recent construction of the Tien Shan inferred from GPS measurements of present-day crustal deformation rates, *Nature*, *384*, 450–453.
- Abdrakmatov, K. Y., R. J. Weldon, S. C. Thompson, D. W. Burbank, C. M. Rubin, M. Miller, and P. Molnar (2001), Onset, style and current rate of shortening in the central Tien Shan (Kyrgyzstan), *Russ. Geol. Geophys.*, *42*, 1502–1526.
- Aizen, V., E. Aizen, and J. Melack (1995), Characteristics of runoff formation at the Kirgizshiy Alatau, Tien Shan, in *Biogeochemistry of Seasonally Snow-Covered Catchments: Proceedings of a Boulder Symposium*, vol. 228, edited by K. Tonnessen, M. Williams, and M. Tranter, pp. 413–430, Int. Assoc. of Hydrol. Sci., Boulder, Colo.
- Amos, C. B., D. W. Burbank, D. C. Nobes, and S. A. L. Read (2007), Geomorphic constraints on listric thrust faulting: Implications for active deformation in the Mackenzie Basin, South Island, New Zealand, *J. Geophys. Res.*, *112*, B03S11, doi:10.1029/2006JB004291.
- Anderson, R. S., P. Molnar, and M. A. Kessler (2006), Features of glacial valley profiles simply explained, *J. Geophys. Res.*, *111*, F01004, doi:10.1029/2005JF000344.
- Benda, L., and T. Dunne (1997), Stochastic forcing of sediment routing and storage in channel networks, *Water Resour. Res.*, *33*, 2865–2880.
- Brocklehurst, S., and K. X. Whipple (2002), Glacial erosion and relief production in the eastern Sierra Nevada, California, *Geomorphology*, *42*, 1–24.
- Brozovic, N., D. R. Burbank, and A. J. Meigs (1997), Climatic limits on landscape development in the northwestern Himalaya, *Science*, *276*, 571–574.
- Bullen, M. E., D. W. Burbank, J. I. Garver, and K. Y. Abdrakmatov (2001), Late Cenozoic tectonic evolution of the northwestern Tien Shan: New age estimates for the initiation of mountain building, *Geol. Soc. Am. Bull.*, *113*, 1544–1559.
- Bullen, M. E., D. W. Burbank, and J. I. Garver (2003), Building the northern Tien Shan: Integrated thermal, structural, and topographic constraints, *J. Geol.*, *111*, 149–165.
- Burbank, D. W., J. Leland, E. Fielding, R. S. Anderson, M. R. Reid, and C. Duncan (1996), Bedrock incision, rock uplift and threshold hillslopes in the northwestern Himalayas, *Nature*, *379*, 505–508.
- Burbank, D. W., L. J. McLean, M. E. Bullen, K. Y. Abdrakmatov, and M. Miller (1999), Partitioning of intermontane basins by thrust-related folding, Tien Shan, Kyrgyzstan, *Basin Res.*, *11*, 75–92.
- Chediya, O. (1986), *Morphostructure and Neo-tectonics of the Tien Shan*, Acad. Nauk Kyrgyz SSR, Frunze, Kyrgyzstan.
- Church, M., and J. M. Ryder (1972), Paraglacial sedimentation: A consideration of fluvial processes conditioned by glaciation, *Geol. Soc. Am. Bull.*, *83*, 3059–3072.
- Crosby, B. T., and K. X. Whipple (2006), Knickpoint initiation and distribution within fluvial networks: 236 waterfalls in the Waipaoa River, North Island, New Zealand, *Geomorphology*, *82*, 16–38.
- Davis, W. M. (1904), A flat-topped range in the Tian-Shan, *Appalachia*, *10*, 277–284.
- Densmore, A. L., N. H. Dawers, S. Gupta, R. Guidon, and T. Goldin (2004), Footwall topographic development during continental extension, *J. Geophys. Res.*, *109*, F03001, doi:10.1029/2003JF000115.
- Densmore, A. L., N. H. Dawers, S. Gupta, and R. Guidon (2005), What sets topographic relief in extensional footwalls?, *Geology*, *33*, 453–456.
- Ellis, M. A., and A. L. Densmore (2006), First-order topography over blind thrusts, in *Tectonics, Climate, and Landscape Evolution*, edited by S. D. Willett et al., pp. 251–266, Geol. Soc. of Am., Boulder, Colo.
- Ellis, M. A., A. L. Densmore, and R. S. Anderson (1999), Development of mountainous topography in the basin ranges, *Basin Res.*, *11*, 21–41.
- England, P., and P. Molnar (1990), Surface uplift, uplift of rocks, and exhumation of rocks, *Geology*, *18*, 1173–1177.
- Gregory, K. M., and C. G. Chase (1994), Tectonic and climatic significance of a late Eocene low-relief, high-level geomorphic surface, Colorado, *J. Geophys. Res.*, *99*, 20,141–20,160.
- Hack, J. (1957), Studies of longitudinal profiles in Virginia and Maryland, *U. S. Geol. Surv. Prof. Pap.*, 294-B.
- Hancock, G. S., R. S. Anderson, and K. X. Whipple (1998), Beyond power: Bedrock river incision process and form, in *Rivers Over Rock: Fluvial Processes in Bedrock Channels*, *Geophys. Monogr. Ser.*, vol. 107, edited by K. J. Tinkler and E. E. Wohl, pp. 35–60, AGU, Washington, D. C.
- Hilley, G. E., P. M. Blisniuk, and M. R. Strecker (2005), Mechanics and erosion of basement-cored uplift provinces, *J. Geophys. Res.*, *110*, B12409, doi:10.1029/2005JB003704.
- Howard, A. D. (1971), Simulation model of stream capture, *Geol. Soc. Am. Bull.*, *82*, 1355–1376.
- Howard, A. D. (1994), A detachment-limited model of drainage basin evolution, *Water Resour. Res.*, *30*, 2261–2285.
- Howard, A. D., and G. Kerby (1983), Channel changes in badlands, *Geol. Soc. Am. Bull.*, *94*, 739–752.
- Humphrey, N. F., and S. K. Konrad (2000), River incision or diversion in response to bedrock uplift, *Geology*, *28*, 43–46.
- Ijjasz-Vasquez, E. J., R. L. Bras, and I. Rodriguez-Iturbe (1993), Hack's relation and optimal channel networks: The elongation of river basins as a consequence of energy minimization, *Geophys. Res. Lett.*, *20*, 1583–1586.
- Jordan, T. E., and R. W. Allmendinger (1986), The Sierras Pampeanas of Argentina: A modern analogue of Rocky Mountains foreland deformation, *Am. J. Sci.*, *286*, 737–764.
- Kirby, E., and K. Whipple (2001), Quantifying differential rock-uplift rates via stream profile analysis, *Geology*, *29*, 415–418.
- Lague, D., N. Hovius, and P. Davy (2005), Discharge, discharge variability, and the bedrock channel profile, *J. Geophys. Res.*, *110*, F04006, doi:10.1029/2004JF000259.
- Lavé, J., and J. P. Avouac (2001), Fluvial incision and tectonic uplift across the Himalayas of central Nepal, *J. Geophys. Res.*, *106*, 26,562–26,591.
- Miller, S. R., R. Slingerland, and E. Kirby (2002), Landscape evolution in orogens with significant lateral advection of rock: Insights from numerical simulations of fault-bend folds, *Eos Trans. AGU*, *83*(47), Fall Meet. Suppl., Abstract T72B-05.
- Molnar, P., and H. Lyon-Caen (1988), Some simple physical aspects of the support, structure, and evolution of mountain belts, in *Processes in Continental Lithospheric Deformation*, edited by S. J. Clarke, *Spec. Pap. Geol. Soc. Am.*, *218*, 179–207.
- Montgomery, D. R., and W. E. Dietrich (1992), Channel initiation and the problem of landscape scale, *Science*, *255*, 826–830.
- Oskin, M. E., and D. W. Burbank (2005), Alpine landscape evolution dominated by cirque retreat, *Geology*, *33*, 933–936.
- Rodgers, J. (1987), Chains of basement uplifts within cratons marginal to orogenic belts, *Am. J. Sci.*, *287*, 661–692.
- Roe, G. H., D. R. Montgomery, and B. Hallet (2003), Orographic precipitation and the relief of mountain ranges, *J. Geophys. Res.*, *108*(B6), 2315, doi:10.1029/2001JB001521.
- Sklar, L., and W. E. Dietrich (1998), River longitudinal profiles and bedrock incision models: Stream power and the influence of sediment supply, in *Rivers Over Rock: Fluvial Processes in Bedrock Channels*, *Geophys. Monogr. Ser.*, vol. 107, edited by K. J. Tinkler and E. E. Wohl, pp. 237–260, AGU, Washington, D. C.
- Sklar, L. S., and W. E. Dietrich (2004), A mechanistic model for river incision into bedrock by saltating bed load, *Water Resour. Res.*, *40*, W06301, doi:10.1029/2003WR002496.
- Snyder, N. P., K. X. Whipple, G. Tucker, and D. J. Merritts (2000), Landscape response to tectonic forcing: Digital elevation model analysis of stream profiles in the Mendocino triple junction area, northern California, *Geol. Soc. Am. Bull.*, *112*, 1250–1263.
- Snyder, N. P., K. X. Whipple, G. E. Tucker, and D. J. Merritts (2003), Importance of a stochastic distribution of floods and erosion thresholds in the bedrock river incision problem, *J. Geophys. Res.*, *108*(B2), 2117, doi:10.1029/2001JB001655.
- Sobel, E. R., G. E. Hilley, and M. R. Strecker (2003), Formation of internally drained contractional basins by aridity-limited bedrock incision, *J. Geophys. Res.*, *108*(B7), 2344, doi:10.1029/2002JB001883.
- Sobel, E. R., M. Oskin, D. Burbank, and A. Mikolaichuk (2006), Exhumation of basement-cored uplifts: Example of the Kyrgyz Range quantified with apatite fission track thermochronology, *Tectonics*, *25*, TC2008, doi:10.1029/2005TC001809.
- Spotila, J. A., K. A. Farley, and K. Sieh (1998), Uplift and erosion of the San Bernardino Mountains associated with transpression along the San Andreas Fault, California, as constrained by radiogenic helium thermochronometry, *Tectonics*, *17*, 360–378.
- Stock, J., and W. E. Dietrich (2003), Valley incision by debris flows: Evidence of a topographic signature, *Water Resour. Res.*, *39*(4), 1089, doi:10.1029/2001WR001057.
- Thompson, S. C., R. J. Weldon, C. M. Rubin, K. Abdrakmatov, P. Molnar, and G. W. Berger (2002), Late Quaternary slip rates across the central Tien Shan, Kyrgyzstan, central Asia, *J. Geophys. Res.*, *107*(B9), 2203, doi:10.1029/2001JB000596.

- Tucker, G. E., and K. X. Whipple (2002), Topographic outcomes predicted by stream erosion models: Sensitivity analysis and intermodel comparison, *J. Geophys. Res.*, *107*(B9), 2179, doi:10.1029/2001JB000162.
- van der Beek, P., B. Champel, and J.-L. Mugnier (2002), Control of detachment dip on drainage development in regions of active fault-propagation folding, *Geology*, *30*, 471–474.
- Whipple, K., and G. E. Tucker (1999), Dynamics of the stream power river incision model: Implications for height limits of mountain ranges, landscape response timescales and research needs, *J. Geophys. Res.*, *104*, 17,661–17,674.
- Whipple, K. X., and G. E. Tucker (2002), Implications of sediment-flux-dependent river incision models for landscape evolution, *J. Geophys. Res.*, *107*(B2), 2039, doi:10.1029/2000JB000044.
- Whipple, K. X., E. Kirby, and S. H. Brocklehurst (1999), Geomorphic limits to climate-induced increases in topographic relief, *Nature*, *40*, 39–43.
- Whipple, K. X., G. S. Hancock, and R. S. Anderson (2000), River incision into bedrock: Mechanics and relative efficacy of plucking, abrasion, and cavitation, *Geol. Soc. Am. Bull.*, *112*, 490–503.
- Willett, S. D., and M. T. Brandon (2002), On steady state in mountain belts, *Geology*, *30*, 175–178.
- Wobus, C. W., B. T. Crosby, and K. X. Whipple (2006), Hanging valleys in fluvial systems: Controls on occurrence and implications for landscape evolution, *J. Geophys. Res.*, *111*, F02017, doi:10.1029/2005JF000406.
-
- D. Burbank, Department of Earth Science, University of California, Santa Barbara, CA 93106, USA. (burbank@crustal.ucsb.edu)
- M. E. Oskin, Department of Geological Sciences, University of North Carolina at Chapel Hill, Mitchell Hall, CB 3315, Chapel Hill, NC 27599-3315, USA. (oskin@unc.edu)